

# Author responses to minor revisions to Biogeosciences manuscript bg-2016-159 "Fate of terrigenous organic matter across the Laptev Sea from the mouth of the Lena River to the deep sea of the Arctic interior"

by Lisa Bröder, Tesi, Salvadó, Semiletov, Dudarev and Gustafsson

We are glad to hear the editor's positive assessment of our revised manuscript, yet have taken the constructive criticism seriously. All comments and our responses, as well as the resulting edits, are detailed below, organized as in the previous response letter: first the reviewer comments are given in italic, directly followed by our response and outline of the resulting edit in regular font. References in our response to line numbers refer to the revised manuscript version (with tracked changes).

## Editor comments

### SPECIFIC POINTS:

- 1) *"L76-78: The order of words seems a bit off to me. Please check the phrasing."*

The original *"The resulting long cross-shelf transport and thereby time spent in oxic sediments might exert first order control on TerrOC degradation..."* has been reworded to *"Protracted cross-shelf transport may hence result in long oxygen exposure times, which might exert first order control on TerrOC degradation..."*

- 2) *"L301: input of young autochthonous material is not supported by the stable carbon isotopic signature – please specify how."*

The explanation has now been added in L302-304: *"However, this latter scenario is not supported by the stable carbon isotopic signature, as values for  $\delta^{13}\text{C}$  increase from about -24.3 ‰ on the mid-shelf to about -22.5 ‰, suggesting a higher fraction of marine organic matter for the deep stations."*

- 3) *"Comment 4 of reviewer 2: I still think this is a valuable comment. Please specify that the transport times reported by Keil et al. (2004) are for an active margin, and should be taken here as a minimum."*

This has been clarified in L290-292.

- 4) *"Add the contribution of the reviewers to the acknowledgements."*

The work of the reviewers has now been acknowledged in L659-661.

- 5) *"Table 1: have d13C measurements done in duplicate? If so, what was the error, and what value is displayed here in the table (average)? What is the precision of the measurement, i.e. can you report d13C values with this amount of significant numbers?"*

The d13C values stem from single measurements. Since the reproducibility of the instrument is <0.15 ‰, there should not be more than three significant digits in the table. This has now been adjusted accordingly.

1 **Fate of terrigenous organic matter across the Laptev Sea**  
2 **from the mouth of the Lena River to the deep sea of the**  
3 **Arctic interior**

4 Lisa Bröder <sup>a,b\*</sup>, Tommaso Tesi <sup>a,b,c</sup>, Joan A. Salvadó <sup>a,b</sup>, Igor P. Semiletov <sup>d,e,f</sup>, Oleg  
5 V. Dudarev <sup>e,f</sup>, Örjan Gustafsson <sup>a,b</sup>

6 <sup>a</sup> *Department of Environmental Science and Analytical Chemistry, Stockholm University,*  
7 *Stockholm, Sweden*

8 <sup>b</sup> *Bolin Centre for Climate Research, Stockholm University, Stockholm, Sweden*

9 <sup>c</sup> *Institute of Marine Sciences – National Research Council, Bologna, Italy*

10 <sup>d</sup> *International Arctic Research Center, University Alaska Fairbanks, Fairbanks, USA*

11 <sup>e</sup> *Pacific Oceanological Institute, Russian Academy of Sciences, Vladivostok, Russia*

12 <sup>f</sup> *Tomsk National Research Politechnical University, Tomsk, Russia*

13 \*corresponding author: [lisa.broder@aces.su.se](mailto:lisa.broder@aces.su.se)

14 **Abstract**

15 Ongoing global warming in high latitudes may cause an increasing supply of permafrost-  
16 derived organic carbon through both river discharge and coastal erosion to the Arctic  
17 shelves. Mobilized permafrost carbon can be either buried in sediments, transported to the  
18 deep sea or degraded to CO<sub>2</sub> and outgassed, potentially constituting a positive feedback to  
19 climate change.

20 This study aims to assess the fate of terrestrial organic carbon (TerrOC) in the Arctic marine  
21 environment by exploring how it changes in concentration, composition and degradation  
22 status across the wide Laptev Sea shelf. We analyzed a suite of terrestrial biomarkers as  
23 well as source-diagnostic bulk carbon isotopes ( $\delta^{13}\text{C}$ ,  $\Delta^{14}\text{C}$ ) in surface sediments from a  
24 Laptev Sea transect spanning more than 800 km from the Lena River mouth (< 10 m water  
25 depth) across the shelf to the slope and rise (2000-3000 m water depth). These data provide  
26 a broad view on different TerrOC pools and their behavior during cross-shelf transport. The  
27 concentrations of lignin phenols, cutin acids and high-molecular weight (HMW) wax lipids  
28 (tracers of vascular plants) decrease by 89-99 % along the transect. Molecular-based  
29 degradation proxies for TerrOC (e.g., the carbon preference index of HMW lipids, the HMW  
30 acids/alkanes ratio and the acid/aldehyde ratio of lignin phenols) display a trend to more  
31 degraded TerrOC with increasing distance from the coast. We infer that the degree of  
32 degradation of permafrost-derived TerrOC is a function of the time spent under oxic  
33 conditions during protracted cross-shelf transport. Future work should therefore seek to  
34 constrain cross-shelf transport times in order to compute a TerrOC degradation rate and  
35 thereby help to quantify potential carbon-climate feedbacks.

## 36 **1 Introduction**

37 Amplified global warming in high latitudes has raised growing concern about potential  
38 positive carbon-climate feedbacks. Arctic soils store about half of the global soil organic  
39 carbon (Tarnocai et al., 2009), with 60 % of this in perennially frozen grounds (Hugelius et  
40 al., 2014). With ongoing climate change these vast carbon reservoirs become increasingly  
41 vulnerable. Mobilization and transport of old terrigenous organic carbon (TerrOC) into the  
42 Arctic Ocean is expected to intensify (Gustafsson et al., 2011) through enhancing river  
43 discharge (McClelland et al., 2008) with augmenting sediment loads (Gordeev, 2006;  
44 Syvitski, 2002) and accelerating coastal erosion (Günther et al., 2013). This material can be  
45 buried in the sediments of the Arctic shelves, transported across the margin towards deeper  
46 basins or degraded and re-introduced into the modern carbon cycle as CO<sub>2</sub>, thereby not only  
47 providing a potential positive feedback to global warming, but also causing severe ocean  
48 acidification (Semiletov et al., 2016). The fate of permafrost-released TerrOC in the marine  
49 environment is thus crucial for future climate projections, yet insufficiently understood (Vonk  
50 and Gustafsson, 2013).

51 The East Siberian Arctic Shelf (ESAS) is with a width of > 800 km the world's largest  
52 continental shelf. It receives TerrOC both from the erosion of the East Siberian shoreline,  
53 largely consisting of organic-rich, late-Pleistocene ice-complex deposits (Yedoma), and via  
54 the Great Russian Arctic Rivers, which drain extensive areas of continuous and  
55 discontinuous permafrost. The Laptev Sea is a representative for the TerrOC dominated  
56 Siberian shelf seas, since its main organic carbon input originates from substantial coastal  
57 erosion (as observed in the Buor-Khaya Bay, Sánchez-García et al., 2011; Semiletov et al.,  
58 2011; Vonk et al., 2012) and the Lena River, the main fluvial sediment source for the entire  
59 ESAS (Holmes et al., 2002).

60 Previous studies have focused on near-shore areas and the inner shelf (e.g. Bröder et al.,  
61 2016; Charkin et al., 2011; Feng et al., 2015; Karlsson et al., 2011; Salvadó et al., 2015;  
62 Sánchez-García et al., 2011; Semiletov et al., 2005, 2012, 2013; Tesi et al., 2014; Vonk et  
63 al., 2010, 2012, 2014; Winterfeld et al., 2015b, 2015a). They reported large fractions of old

64 TerrOC in particulate organic carbon (POC) and surface sediments close to the coast, using  
65 different approaches such as applying carbon-isotope-based source apportionment (e.g.  
66 Gustafsson et al., 2011; Semiletov et al., 2005; Vonk et al., 2010, 2012, 2014; Salvadó et al.,  
67 2015, for the iron-associated OC fraction in the sediment) and by analyzing terrigenous  
68 biomarkers in both surface sediments (e.g. Feng et al., 2013; Stein and Macdonald, 2004;  
69 Tesi et al., 2014, 2016) and POC in the water column (e.g. Charkin et al., 2011; Karlsson et  
70 al., 2011; Winterfeld et al., 2015a). This is the first study that encompasses sampling stations  
71 along the entire transect from the Lena River mouth, across the wide Laptev Sea shelf, to the  
72 continental slope and rise. Our major objective was to gain new insights regarding the  
73 behavior of different TerrOC pools, in particular investigating potential degradation of  
74 permafrost-released material along the land-shelf-basin continuum. The Laptev Sea and  
75 adjacent East Siberian Sea are among the widest continental margins on Earth (Jakobsson  
76 et al., 2004). Protracted cross-shelf transport may hence result in long oxygen exposure  
77 times, which ~~The resulting long cross-shelf transport and thereby time spent in oxic~~  
78 ~~sediments~~ might exert first order control on TerrOC degradation (e.g. Keil et al., 2004). Our  
79 study area is thus well suited to test hypotheses on the fate of permafrost carbon in terms of  
80 carbon-climate feedback. We have therefore characterized TerrOC in surface sediments  
81 along the Laptev Sea transect on both bulk and molecular level, exploiting source-diagnostic  
82 bulk carbon isotopes ( $\delta^{13}\text{C}$ ,  $\Delta^{14}\text{C}$ ) as well as an extensive biomarker suite (lignin phenols and  
83 cutin acids obtained by alkaline CuO oxidation and high-molecular-weight solvent-extractable  
84 lipids, such as *n*-alkanes and *n*-alkanoic acids).

## 85 **2 Material and Methods**

### 86 2.1 Study area

87 The Laptev Sea is the shallowest of the Arctic shelf seas with an average depth of 48 m  
88 (Jakobsson et al., 2004). It spans over 498,000 km<sup>2</sup> with a volume of 24,000 km<sup>3</sup> and is  
89 located between the Kara Sea and Severnaya Zemlya in the West and the East Siberian Sea  
90 and the New Siberian Islands in the East. The main sources of particulate organic carbon  
91 (POC) for the Laptev Sea are terrigenous, both from coastal erosion and river runoff  
92 (Sánchez-García et al., 2011; Stein and Macdonald, 2004). Marine primary production is  
93 limited to on average two ice-free months per year and therefore generally low. Nutrient-poor  
94 waters on the Siberian shelves resulting from a strong stratification further impede  
95 phytoplankton growth (Sakshaug, 2004).

96 The destabilization of Pleistocene Ice-Complex Deposits along the coastline is a main  
97 sediment source for the Laptev Sea (Rachold et al., 2000). The total POC input from coastal  
98 erosion to Laptev and East Siberian Sea is estimated to be between 4.0 Tg yr<sup>-1</sup> (Semiletov,  
99 1999; Stein and Fahl, 2000) and 22 ± 8 Tg yr<sup>-1</sup> (including net subsea permafrost-carbon  
100 erosion, Vonk et al., 2012).

101 The Lena River is estimated to provide 20.7 Tg of sediment per year (Holmes et al., 2002),  
102 i.e. > 70 % of the total riverine input to the Laptev Sea (Gordeev, 2006) with an average water  
103 discharge of 588 km<sup>3</sup> yr<sup>-1</sup> (Holmes et al., 2012). It drains a watershed of ~2.46 x 10<sup>6</sup> km<sup>2</sup>  
104 (Holmes et al., 2012), of which 77 % is underlain by continuous permafrost (Amon et al.,  
105 2012). Water discharge peaks in June, during the spring flood, when about 75 % of total  
106 organic carbon is delivered (Rachold et al., 2004). Total POC discharge by the Lena River  
107 can be up to 0.38 Tg yr<sup>-1</sup> (Semiletov et al., 2011).

108 Sediment transport pathways are largely influenced by the prevailing atmospheric conditions:  
109 During cyclonic summers (i.e. positive phase of the Arctic Oscillation), northerly winds  
110 predominate, strengthening the Siberian Coastal Current, which transports Lena River water  
111 masses along the coast towards the East Siberian Sea; whereas during anticyclonic  
112 summers (i.e. negative phase of the Arctic Oscillation and mainly southerly winds) the Lena

113 River plume is exported onto the mid-shelf and towards the deep part of the Arctic Ocean  
114 (Charkin et al., 2011; Dmitrenko et al., 2008; Guay et al., 2001; Wegner et al., 2013;  
115 Weingartner et al., 1999). Sediment transport in the Laptev Sea is strongly seasonal. The  
116 main transport of Lena River water with high concentrations of suspended particulate matter  
117 (SPM) towards the mid-shelf takes place shortly after river-ice breakup (Wegner et al., 2005).  
118 During the ice-free summer, SPM circulates between inner and mid-shelf with very little  
119 material escaping over the shelf break to the deeper parts of the Arctic Ocean. Significant  
120 sediment export is suggested to happen during freeze-up through SPM that is incorporated  
121 in sea ice and then transported across the continental margin (Dethleff, 2005; Eicken et al.,  
122 1997) or through the formation of dense bottom water resulting from brine ejection (Dethleff,  
123 2010; Ivanov and Golovin, 2007). Hardly any sediment transport occurs beneath the ice  
124 cover.

125 Holocene-scale linear sedimentation rates for the Laptev Sea vary between 0.12 and 0.59  
126 mm yr<sup>-1</sup> according to <sup>14</sup>C dating of marine bivalves (Stein and Fahl, 2004, and citations  
127 therein), whereas centennial-scale <sup>210</sup>Pb-derived rates for the more recent Laptev Sea can  
128 be up to 1.3 mm yr<sup>-1</sup> (Vonk et al., 2012). These rates do not seem to be correlated with water  
129 depth on the shelf, but values for the continental slope and rise tend to be on the lower end  
130 (0.12-0.38 mm yr<sup>-1</sup>) (Stein and Fahl, 2004, and citations therein).

131

## 132 2.2 Sampling

133 Sediment sampling locations span from close to the Lena River mouth and in the Buor-  
134 Khaya Bay, across the shelf, to the continental slope and rise, covering a transect of > 800  
135 km with water depths increasing by more than two orders of magnitude. Samples SW-1, SW-  
136 2, SW-3, SW-4, SW-6, SW-14, SW-23 and SW-24 were collected during the SWERUS-C3  
137 expedition on IB *ODEN* during summer 2014 using an Oktopus multicorer (8 Plexiglas tubes,  
138 10 cm diameter). All other samples were collected during the International Siberian Shelf  
139 Study (ISSS-08) expedition onboard the RV *Yacob Smirnitskyi* during summer 2008. The  
140 YS-4, YS-6, YS-13 and YS-14 samples were taken with a GEMAX gravity corer (2 Plexiglas

141 tubes, 9 cm diameter); YS-9 and TB-46 were collected with a Van Veen grab sampler. For  
142 the grab samples only surface sediments (uppermost cm) were subsampled and used in this  
143 study. Sediment cores were cut into 1 cm slices within 24 hours after sampling. To account  
144 for lower sediment accumulation rates on the rise, for SW-1, SW-2, SW-3 and SW-4 a higher  
145 resolution of 0.5 cm for the top 10 cm was chosen. The depositional age for all samples is  
146 thus between ~8 and ~70 years (depending on which sedimentation rates are employed). All  
147 samples were kept frozen throughout the expedition and freeze-dried upon arrival to  
148 Stockholm University laboratories. See Semiletov and Gustafsson (2009) for more  
149 information on the ISSS-08 expedition. For exact sampling locations see Table 1.

150

### 151 2.3 Surface area

152 All surface area analyses have been performed on a Micromeritics Gemini VII Surface Area  
153 and Porosity analyzer. Freeze-dried subsamples of ~0.7 g were furnace at 400 °C for 12 h  
154 and gently cooled down to room temperature to remove all organic material. Keil and Cowie  
155 (1999) have shown that this method yields statistically similar results to the method using  
156 removal with sodium pyrophosphate/ hydrogen peroxide (Mayer, 1994). The samples were  
157 then desalted by repeated mixing with 50 ml of MilliQ water and centrifugation (20 min at  
158 8000 rpm), followed by further freeze-drying. Directly prior to analysis they were degassed in  
159 a Micromeritics FlowPrep 060 Sample Degas System for 2 h at 200 °C under a constant  
160 nitrogen flow. Each analysis was initiated by measuring the free space in the vial. The  
161 specific surface areas were derived from 6 pressure-point measurements (relative pressure  
162  $p/p_0 = 0.05-0.3$ , equilibration time 5 s) with nitrogen as adsorbing gas (Brunauer et al., 1938).  
163 The instrumental precision was  $0.1-0.3 \text{ m}^2 \text{ g}^{-1}$ , which corresponds to a relative uncertainty of  
164 about 1 %. The performance of the instrument was monitored with the surface area  
165 reference material Carbon Black ( $21.0 \pm 0.75 \text{ m}^2 \text{ g}^{-1}$ ) provided by Micromeritics.

166

### 167 2.4 X-Ray Fluorescence



168 The mineral composition of ~1 g freeze-dried, homogenized subsamples was also  
169 characterized with a wavelength dispersive sequential Philips PW2400 X-ray Fluorescence  
170 (XRF) spectrometer. Prior to the analysis, sediment samples were combusted for 12h at 450  
171 °C to remove the organic fraction. The XRF was operated under vacuum conditions on  
172 samples prepared as glass beads using lithium tetraborate and melted with a fluxer Claisse  
173 Fluxy (~1150°C) (Mercone et al., 2001). The relative error was less than 0.6 % for major  
174 elements and less than 3 % for trace elements. In this study only SiO<sub>2</sub>, Al<sub>2</sub>O<sub>3</sub> and CaO are  
175 reported.

176

## 177 2.5 Bulk elemental and carbon isotope analysis

178 Concentration and  $\delta^{13}\text{C}$  isotopic composition of total organic carbon (TOC) were determined  
179 at the Stable Isotope Laboratory, Department of Geological Sciences, Stockholm University.  
180 Homogenized subsamples of ~10 mg were repeatedly acidified (HCl, 1.5 M, Ag capsules) to  
181 remove carbonates (Nieuwenhuize et al., 1994). TOC concentrations and  $\delta^{13}\text{C}$  isotopic  
182 composition were measured simultaneously with a Carlo Erba NC2500 elemental analyzer  
183 connected via a split interface to a Finnigan MAT Delta V mass spectrometer. TOC  
184 concentrations were blank corrected and the relative error was < 1 %. Stable isotope data  
185 are reported relative to VPDB using the  $\delta^{13}\text{C}$  notation.

186 Radiocarbon analyses of acidified samples were conducted at the US National Ocean  
187 Sciences Accelerator Mass Spectrometry (NOSAMS) Facility of the Woods Hole  
188 Oceanographic Institution, USA, according to their standard routines (Pearson et al., 1998).  
189 The relative error of the measurements was < 0.5 %. Radiocarbon data are reported using  
190 the  $\Delta^{14}\text{C}$  notation following Stuvier and Polach (1977).

191

## 192 2.6 Biomarkers

### 193 2.6.1 CuO-oxidation products

194 Microwave-assisted alkaline CuO oxidation was performed according to the method  
195 established by Goñi and Montgomery (2000). Homogenized subsamples of 100-400 mg of

196 sediment (corresponding to 2-5 mg OC) were combined with 300 mg of copper(II) oxide and  
197 50 mg of ferrous ammonium sulfate and oxidized under oxygen-free conditions (degassed  
198 NaOH, 8 wt %) at 150 °C for 90 min using an UltraWAVE Milestone 215 Microwave oven.  
199 After oxidation, known amounts of trans-cinnamic acid and ethyl vanillin were added as  
200 recovery standards. Samples were acidified to pH 1 with HCl (12 M) and repeatedly  
201 extracted with ethyl acetate. Anhydrous Na<sub>2</sub>SO<sub>4</sub> was added to remove remaining water. The  
202 solvent was evaporated and extracts re-dissolved in pyridine. For quantification, subsamples  
203 were derivatized with bis-trimethylsilyl-trifluoroacetamide (BSTFA) + 1 %  
204 trimethylchlorosilane (TMCS) and analyzed on a gas-chromatograph mass spectrometer in  
205 full scan mode (GC-MS, Agilent) using a DB5-MS capillary column (60 m x 250 µm, 0.25 µm  
206 stationary phase thickness, Agilent J&W) with a temperature profile of initially 60 °C followed  
207 by a ramp of 5 °C min<sup>-1</sup> until reaching and holding 300 °C for 5 min. The quantification of  
208 lignin phenols, benzoic acids, and p-hydroxybenzenes was achieved by comparison to the  
209 response factors (key ions) of commercially available standards. For cutin-derived products,  
210 fatty acids and dicarboxylic acids the response factor of trans-cinnamic acid was used as in  
211 Goñi et al. (1998).

212

### 213 2.6.2 Solvent-extractable lipids

214 Wax lipids were extracted by means of accelerated solvent extraction (Dionex ASE 300)  
215 using dichloromethane:methanol (9:1) according to the method described by Wiesenberg et  
216 al. (2004). Pre-rinsed stainless-steel vessels were loaded with ~3 g of freeze-dried sediment,  
217 filled up with pre-combusted glass beads and pre-combusted glass fiber filters at both ends.  
218 Two extraction cycles were performed per sample applying a static pressure of 1500 psi and  
219 a temperature of 80 °C for 5 min after a heating phase of 5 min. The flush volume was 50 %  
220 of the 34 ml cell size with a purging time of 100 s.

221 Extracts were further purified (addition of activated Cu for sulfur and anhydrous Na<sub>2</sub>SO<sub>4</sub> for  
222 water removal) and then separated into a neutral and an acid fraction using BondElut  
223 cartridges (bonded phase NH<sub>2</sub>, Varian), eluting with dichloromethane:isopropanol (2:1) for

224 the neutral and methyl *tert*-butyl ether with 4 % acetic acid for the acid fraction according to  
225 the method described by van Dongen et al. (2008a). The neutral fraction was further  
226 separated into a polar and a non-polar fraction with an Al<sub>2</sub>O<sub>3</sub> column. For each of the three  
227 compound classes *n*-alkanes (neutral non-polar fraction), *n*-alkanols (neutral polar fraction)  
228 and *n*-alkanoic acids (acid fraction) ~10 mg of one internal standard, d<sub>50</sub>-tetracosane, 2-  
229 hexadecanol and d<sub>39</sub>-eicosanoic acid respectively, were added to the sediment samples prior  
230 to extraction. All fractions were then analyzed on a GC–MS (Agilent) using the same column  
231 and temperature program as for the CuO products. The polar and acid fractions were  
232 derivatized with BSTFA + 1 % TMCS prior to analysis. Quantification was performed using a  
233 5-point calibration curve with commercially available standards. Here, we only report data for  
234 high-molecular weight (HMW) *n*-alkanes and *n*-alkanoic acids, where HMW refers to carbon  
235 chain-lengths of ≥ 23 for *n*-alkanes and ≥ 24 for *n*-alkanoic acids.

### 236 **3 Results and Discussion**

237 The fate of permafrost-released terrigenous organic carbon (TerrOC) across the Laptev Sea  
238 shelf is controlled by competing processes. Degradation and sorting, as well as replacement  
239 of TerrOC by autochthonous marine organic matter all co-occur to varying degrees during  
240 cross-shelf transport. To disentangle their effects on the fate of permafrost-released TerrOC  
241 we first report changes in bulk sediment and OC properties and then focus on differences on  
242 the molecular level.

243

#### 244 3.1 Characterization of the transect on a bulk level

245 Bulk total organic carbon (TOC) concentrations decreased across the shelf with highest  
246 values (~2 %) at shallow water depths and lowest values on the shelf edge (~0.8 %); at high  
247 water depths (> 2000 m) concentrations were slightly higher (~1 %). TOC values and the  
248 general pattern were in accordance with previous data from the Laptev Sea (Semiletov et al.,  
249 2005; Shakhova et al., 2015; Stein and Fahl, 2004; Vonk et al., 2012) and within the same  
250 range of those measured for the North American Arctic margin (Goni et al., 2013).

251 Normalizing TOC concentrations to the mineral-specific surface area (SA) helps to  
252 understand the influence of physical sorting and preferential deposition on the observed TOC  
253 trends since SA is correlated to the sediment grain size to a first order approximation. To test  
254 if the mineral surface area is altered by the input of autochthonous organisms with siliceous  
255 or carbonaceous skeleton (e.g. silicoflagellates/diatoms or foraminifera/shells respectively),  
256 the mineral composition of the sediments was examined by X-ray fluorescence analysis.

257 There were no apparent trends with water depth for either  $\text{SiO}_2/\text{Al}_2\text{O}_3$  or  $\text{CaO}/\text{Al}_2\text{O}_3$ ;  
258 therefore, marine production is not expected to have a measureable effect and SA can thus  
259 be regarded as a conservative parameter. This was also confirmed by low biogenic silica  
260 concentrations for the Laptev Sea reported earlier (< 1.4 %, Mammone, 1998).

261 The relationship between TOC and SA has been widely studied on continental margins (e.g.  
262 Blair and Aller, 2012; Keil et al., 1994; Mayer, 1994). The TOC/SA ratios of typical river  
263 suspended sediments range between 0.4 and 1  $\text{mg m}^{-2}$  (Mayer, 1994). TOC/SA ratios > 1

264 mg m<sup>-2</sup> have been found in areas with high TOC supply (e.g. river outlets) and where the  
265 deposited organic matter had spent little time under oxic conditions (short oxygen exposure  
266 time, OET) (Mayer et al., 2002). Ratios < 0.4 mg m<sup>-2</sup> generally correspond to sediments from  
267 deeper parts of the ocean and long OETs (e.g. Aller and Blair, 2006). Accordingly, the  
268 TOC/SA values along the Laptev Sea transect displayed a strong decrease from 2.2 and 1.7  
269 mg m<sup>-2</sup> close to the Lena River delta (water depths of 11 and 7 m, respectively) to about 0.3  
270 mg m<sup>-2</sup> at water depths greater than 2000 m (Fig. 2A), proposing extensive TOC loss during  
271 cross-shelf transport.

272 Bulk TOC isotopes have been broadly used to distinguish between organic matter sources.  
273 Radiocarbon isotopes (<sup>14</sup>C) convey information about the age of organic material, with  
274 younger OC having higher  $\Delta^{14}\text{C}$  values. Marine organic matter produced primarily from CO<sub>2</sub>  
275 is expected to have modern <sup>14</sup>C signatures, whereas permafrost-derived TerrOC has aged  
276 both on land and during transport and has thus more depleted <sup>14</sup>C values. The  $\Delta^{14}\text{C}$  values  
277 for our Laptev Sea transect were generally low (< -280 ‰, Fig. 2B), suggesting a significant  
278 input of pre-aged TerrOC (as in Vonk et al., 2012). Bulk TOC showed less depleted  $\Delta^{14}\text{C}$   
279 signatures with increasing distance from land on the shelf (from about -500 ‰ to about -340  
280 ‰ on the outer shelf, Fig. 2B), reflecting a dilution of older TerrOC with younger marine  
281 material. On the slope and rise, however,  $\Delta^{14}\text{C}$  values decreased again to about -410 ‰.  
282 This difference may be a result of ageing during lateral transport and/or after deposition due  
283 to lower accumulation rates on slope and rise. The range between -340 ‰ and -410 ‰  
284 corresponds to a  $\Delta^{14}\text{C}$  age difference of about 900 years; however, the depositional age  
285 differences between shelf and slope samples were estimated to be less than 80 years (see  
286 Section 2.2). Ageing after burial alone does therefore not explain the difference in  $\Delta^{14}\text{C}$ . Keil  
287 et al. (2004) estimated a lateral transport time of 1800 years across the Washington margin  
288 (158 km) from  $\Delta^{14}\text{C}$  data of bulk OC in surface sediments. For the > 200 km distance  
289 between mid-shelf and rise a bulk ageing of 900 years does therefore not seem

290 | unreasonable, particularly since the Washington margin, as opposed to the Laptev Sea shelf,  
291 | is an active margin. The value from Keil et al. (2004) may therefore be regarded as a lower

292 | boundary. It has to be taken into account, however, that mainly the TerrOC fraction of the  
293 bulk OC is subject to such protracted lateral transport. Transport times would thus have to be  
294 significantly higher in order to explain this age difference for the entire bulk OC. One  
295 indication supporting this hypothesis of protracted lateral transport of TerrOC is the  
296 degradation status of TerrOC at the deep stations. All molecular degradation proxies point  
297 towards highly reworked material (see Section 3.3), suggesting that only the most refractory  
298 TerrOC fraction is found at great water depths off the continental margin. Alternatively, the  
299 lower  $\Delta^{14}\text{C}$  values at high water depths may be the consequence of more effective  
300 degradation of marine organic matter throughout the water column, resulting in a  
301 comparatively lower input of young autochthonous material. However, this latter scenario is  
302 not supported by the stable carbon isotopic signature, as values for  $\delta^{13}\text{C}$  increase from about  
303 -24.3 ‰ on the mid-shelf to about -22.5 ‰, suggesting a higher fraction of marine organic  
304 matter for the deep stations.

305 For stable carbon isotopes ( $^{13}\text{C}$ ), terrigenous sources are generally more depleted than  
306 marine organic matter (Fry and Sherr, 1984). In this study, values for  $\delta^{13}\text{C}$  of TOC ranged  
307 between -26.5 ‰ and -22.3 ‰. The trend towards more enriched TOC with increasing  
308 distance from the coast (Fig. 2B) can be explained by a growing proportion of marine organic  
309 matter. However, the  $\delta^{13}\text{C}$  signature of the marine source appeared to be heavier than typical  
310 marine planktonic material in that region ( $-26.7 \pm 1.2$  ‰, Panova et al., 2015;  $-24 \pm 3$  ‰,  
311 Vonk et al., 2012, and citations therein). One possible explanation for this discrepancy is an  
312 underestimated influence of ice algae that were reported to have highly enriched  $\delta^{13}\text{C}$  values  
313 between -15 to -18 ‰ (Schubert and Calvert, 2001). Significant seafloor deposition of ice  
314 algal biomass has been observed previously for the Arctic basins (Boetius et al., 2013).  
315 Another option would be a more refractory, isotopically-enriched marine endmember (-21.2  
316 ‰) as suggested by Magen et al. (2010). They argue that lighter isotopes are preferentially  
317 consumed by bacteria, which in turn enriches the remaining marine organic matter. Following  
318 their reasoning, the more enriched values observed for this transect may be interpreted as  
319 an increasing proportion of refractory marine organic matter.

320 Winterfeld et al. (2015b) analyzed surface water particulate organic carbon (POC) in the  
321 Lena River delta and found a mean  $\delta^{13}\text{C}$  of  $-29.6 \pm 1.5$  ‰. Karlsson et al. (2011) reported  
322 similarly depleted  $\delta^{13}\text{C}$  values for POC from the Buor-Khaya Bay ( $-29.0 \pm 2.0$  ‰), while their  
323 mean value for sedimentary OC for the same stations was significantly more enriched ( $-25.9$   
324  $\pm 0.4$  ‰) and agreed well with our data for the shallow stations ( $-26.2 \pm 0.3$  ‰, stations YS-  
325 13, YS-14 and TB-46). Lena River POC  $\delta^{13}\text{C}$  values from high-discharge periods agree well  
326 with the more enriched values we found for the shallow stations (Rachold and Hubberten,  
327 1998). Stein and Fahl (2004), Semiletov et al. (2011, 2012) and Vonk et al. (2012) presented  
328 similar  $\delta^{13}\text{C}$  ranges and trends for sediments from parts of the Laptev Sea as is reported in  
329 the current study for the entire width of the Laptev Sea shelf. For the Arctic Amerasian  
330 Continental shelf, Naidu et al. (2000) reported contrasts in absolute  $\delta^{13}\text{C}$  values comparing  
331 surface sediment samples from different regions, but all commonly displayed an increasing  
332 trend for  $\delta^{13}\text{C}$  values across the shelf, suggesting a growing fraction of marine organic matter  
333 with increasing distance from the coast.

334 Combining TOC/SA ratios with stable isotope signatures ( $\delta^{13}\text{C}$ ) may serve to disentangle two  
335 different processes, which occur synchronously during cross-shelf transport (as in Keil et al.  
336 1997a): 1.) The net loss of TerrOC and 2.) the replacement of TerrOC with autochthonous  
337 marine OC. Net loss of TerrOC, caused by either degradation or hydrodynamic sorting during  
338 transport, has been quantified previously using TOC/SA ratios (e.g. Aller and Blair, 2006; Keil  
339 et al., 1997a). The carrying-capacity of inorganic particles for OC is assumed to be a function  
340 of the SA (Mayer, 1994); a decrease in TOC/SA values can therefore be regarded as TOC  
341 net loss.

342 Replacement of TerrOC with autochthonous marine OC does not change this ratio. But since  
343 marine OC is known to be isotopically enriched in  $\delta^{13}\text{C}$  over TerrOC, this process is recorded  
344 by an increasing isotopic signature. Along the Laptev Sea transect, both processes seemed  
345 to play an important role (Fig. 2C). High TOC/SA values close to the Lena River decreased  
346 sharply outbound in the nearshore regime, pointing to extensive net loss, while the increase  
347 in  $\delta^{13}\text{C}$  values was minor in this area. Once TOC/SA ratios were  $< 0.8 \text{ mg m}^{-2}$  (water depths

348 > 20 m), the isotopic changes and thus the replacement of TerrOC with marine OC became  
349 increasingly important. Similar trends were observed for the Amazon River delta (Keil et al.,  
350 1997b).  
351 However, the TOC/SA trend in the shallower sediments is likely driven by both degradation  
352 of OC bound to the mineral matrix during cross-shelf transport and sorting of vascular plant  
353 fragments that are retained in the inner shelf. A recent study (Tesi et al., 2016) has shown  
354 that ~50 % of the total OC pool in the inner Laptev shelf surface sediments exists in the form  
355 of large vascular plant fragments. They are trapped close to the coast due to their size and  
356 resulting settling (Stoke's law), while the OC bound to the fine mineral matrix is more buoyant  
357 and transported offshore towards deeper waters.

358

## 359 3.2 Molecular indicators of organic matter sources

### 360 3.2.1 Biomarker distributions

361 The abundances of different source-diagnostic molecular proxies have been extensively  
362 investigated to elucidate complex carbon-cycling mechanisms. In this study, a biomarker  
363 suite of CuO oxidation products and solvent-extractable lipids was analyzed in order to gain  
364 more insights on TerrOC sources and degradation status along the Laptev Sea transect. All  
365 biomarker concentrations were normalized to the sediment-specific surface area (SA)  
366 instead of OC content to avoid the signals being overshadowed by other carbon pools. As  
367 shown by the lack of water-depth-related changes in the mineral composition (Section 3.1),  
368 mineral-matrix dilution by biogenic material is negligible.

369 Lignin-derived phenols have been widely used to trace TerrOC in the marine environment  
370 (e.g. Ertel and Hedges, 1984; Goñi and Hedges, 1995; Hedges and Mann, 1979). The lignin  
371 macro-molecule is only synthesized in vascular plants (and certain seaweed species that are  
372 not existing in the study area) to render stability to the cell walls. Lignin-derived phenols are  
373 typically grouped by phenol type (V: vanillyl phenols, i.e. vanillin, acetovanillone, and vanillic  
374 acid; S: syringyl phenols, i.e. syringaldehyde, aceto syringone, and syringic acid; C: cinnamyl  
375 phenols, i.e. p-coumaric and ferulic acids). Total lignin refers to the sum of the three groups.



376 Across the shelf, lignin loadings decreased substantially with increasing distance from the  
377 coast/water depth ( $45 \mu\text{g m}^{-2}$  close to the coast,  $0.43 \pm 0.09 \mu\text{g m}^{-2}$  for the deep stations; loss  
378 of  $99.1 \pm 0.2 \%$ , Fig. 3A).

379 Cutin-derived hydroxy fatty acids are another compound class obtained from CuO oxidation,  
380 which have been used in parallel with lignin phenols (e.g. Goñi et al., 2000; Prahl et al.,  
381 1994). They are mainly associated with the soft tissues of vascular plants such as leaves and  
382 needles. Cutin acid loadings displayed a similar trend as lignin phenols ( $11 \mu\text{g m}^{-2}$  close to  
383 the coast,  $0.061 \pm 0.010 \mu\text{g m}^{-2}$  for the deep stations; loss of  $99.4 \pm 0.1 \%$ , Fig. 3A).

384 Similar values and sharp declines with increasing distance from the coast for lignin and cutin  
385 have been observed for the whole East Siberian Arctic Shelf (ESAS) (Tesi et al., 2014) (Fig.  
386 4 for comparison of lignin phenol concentrations with literature values for different Arctic  
387 margins). A recent study (Winterfeld et al., 2015a) for the Buor-Khaya Bay (5.8-17 m water  
388 depth) reported lignin phenol concentrations on the same order of magnitude, up to 40 %  
389 higher for the shallowest samples, and decreasing with increasing depth. For the Beaufort  
390 Sea shelf, Goñi et al. (2000) found a less drastic decline in lignin phenols and cutin acids  
391 going from 5 m water depth to 210 m, which likely reflected both lower concentrations in the  
392 shallow waters (factor of  $\sim 2$ ), and a narrower and steeper shelf. Lignin phenols were also  
393 higher at greater water depths than on the ESAS. This may reflect the differences in  
394 bathymetry: since the Beaufort Sea shelf is not as wide as, but steeper than, the ESAS,  
395 lateral transport is possibly faster, leaving less time for organic matter to be degraded along  
396 the way. A comparison between different shelf-slope systems across the North American  
397 Arctic margin (Goni et al., 2013) revealed very low lignin and cutin concentrations for the  
398 Canadian Archipelago, Lancaster Sound and Davis Strait, whereas both concentrations and  
399 trends with water depth for the Beaufort Sea, Chuckchi Sea and Bering Sea were similar to  
400 the results from this study. An exception to these patterns was Barrow Canyon, where at  
401 water depths of  $> 2000$  m lignin and cutin concentrations were as high as the ones observed  
402 close to the Lena River delta, pointing to efficient rapid TerrOC transfer with comparably

403 short oxygen exposure times through this active canyon (Goni et al., 2013) (Fig. 4 and Fig.  
404 S1).

405 Solvent extractable high-molecular weight (HMW) *n*-alkanes and *n*-alkanoic acids make up  
406 the major part of epicuticular leaf waxes (Eglinton and Hamilton, 1967) and have been  
407 broadly employed as TerrOC biomarkers (for the Arctic Ocean e.g. van Dongen et al., 2008;  
408 Yunker et al., 1995, 2005). HMW wax lipids in this study also presented a decreasing trend  
409 with increasing water depth/distance from the coast, but to a lesser extent than lignin phenols  
410 or cutin acids (HMW *n*-alkanes:  $1.1 \mu\text{g m}^{-2}$  close to the coast,  $0.12 \pm 0.02 \mu\text{g m}^{-2}$  for the deep  
411 stations; HMW *n*-alkanoic acids:  $12 \mu\text{g m}^{-2}$  close to the coast,  $0.42 \pm 0.29 \mu\text{g m}^{-2}$  for the deep  
412 stations; loss of  $89 \pm 2 \%$  and  $96 \pm 3 \%$ , respectively, Fig. 3B).

413 Previous studies in the same area reported similar lipid biomarkers concentrations, which  
414 confirm the magnitude of the decreasing trends with increasing water depth (Karlsson et al.,  
415 2011; Vonk et al., 2010) (Fig. S1). HMW *n*-alkane concentrations in the Beaufort and the  
416 Chuckchi Sea (Belicka et al., 2004; Yunker et al., 1993) are in accordance with the ones  
417 measured on the ESAS, but the shallowest sample on the Beaufort Shelf is ~2 times lower  
418 than the shallow ESAS samples (Fig. S1). This might imply that sediments transported by the  
419 Mackenzie River to the Beaufort Shelf have lower TerrOC concentrations than Lena River  
420 transported sediments. For the Mackenzie Shelf, Goñi et al. (2000) used lignin phenols and  
421 cutin acids to estimate a terrigenous  $\delta^{13}\text{C}$  endmember and therewith derived a terrigenous  
422 contribution of almost 80 % for the shallowest sediments, while rough estimates from C/N  
423 and  $\delta^{13}\text{C}$  data suggested that TerrOC made up only 30-50 % of the organic carbon  
424 (Macdonald et al., 2004). For the Lena Delta, source apportionment calculations using  $\delta^{13}\text{C}$   
425 and  $\Delta^{14}\text{C}$  data attributed up to 83 % of the organic carbon to terrigenous sources (Vonk et al.,  
426 2012).

427 All TerrOC biomarker loadings displayed a strong decrease across the shelf, but their relative  
428 losses differ substantially between compound classes (Fig. 3C). These findings agree with  
429 previous results for the ESAS (Tesi et al., 2014), where similar differences between  
430 biomarkers were reported. A somewhat larger decrease was observed for lignin than for

431 cutin, in contrast to this study. The different extents of biomarker losses for the different  
432 compound classes may either be attributed to preferential degradation of lignin phenols and  
433 cutin acids, implying that they are more labile than HMW *n*-alkanes and *n*-alkanoic acids, or  
434 sorting during transport, suggesting that they are associated with a sediment fraction that is  
435 hydraulically more retained and carried less efficiently to the outer shelf/slope. A recent study  
436 (Tesi et al., 2016) aimed to disentangle these two processes by analyzing different fractions  
437 of bulk surface sediments from three transects (yet with only three stations each) across the  
438 ESAS. The fractions were separated according to density ( $1.8 \text{ g cm}^{-3}$  cutoff), size ( $>63 \text{ }\mu\text{m}$ ,  
439  $38\text{-}63 \text{ }\mu\text{m}$ ,  $< 38 \text{ }\mu\text{m}$ ) and settling velocity ( $1 \text{ m d}^{-1}$  cutoff). The highest lignin phenol  
440 abundance was found in low-density plant fragments ( $26\text{-}55 \text{ mg g}^{-1} \text{ OC}$ ). These large  
441 particles have a higher settling velocity (Stokes' law) and are therefore hydraulically retained  
442 close to the coast. Cutin acids and plant wax lipids were mainly associated with the high-  
443 density fine ( $< 38 \text{ }\mu\text{m}$ ,  $> 1 \text{ m d}^{-1}$ ) and ultrafine ( $< 38 \text{ }\mu\text{m}$ ,  $< 1 \text{ m d}^{-1}$ ) mineral fractions. Within  
444 the fine and ultrafine fractions, which made up about 95 % of the organic carbon on the outer  
445 shelf, they found drastic losses of all biomarkers with increasing distance from the coast,  
446 which they attributed to degradation during the protracted cross-shelf transport. Relative  
447 decreases appeared to depend on the number of functional groups of the compound class:  
448  $98 \pm 1 \%$  for lignin phenols,  $97 \pm 1 \%$  for cutin acids,  $96 \pm 1 \%$  for HMW *n*-alkanoic acids and  
449  $89 \pm 4 \%$  for HMW *n*-alkanes. According to that study, the steep cross-shelf gradients  
450 observed here for lignin phenols can be attributed to both hydrodynamic sorting close to the  
451 coast and degradation during transport. From the data in the current study alone, the two  
452 processes occurring in parallel - degradation and sorting during cross-shelf transport - cannot  
453 be disentangled. However, using the data from (Tesi et al., 2016), we can make a rough  
454 correction for the sorting part to derive an estimate of the net extent of degradation. For the  
455 shallowest station in their study (same as here, TB-46), about 75 % of the lignin phenols  
456 were associated with the low density fraction that was retained close to the coast. If we thus  
457 assume only 25 %, i.e. 11 of the  $45 \text{ }\mu\text{g m}^{-2}$  to be associated with the fine fraction that is  
458 actually transported across the shelf, we obtain a reduction by  $96 \pm 1 \%$  that can be

459 attributed to degradation (compared to 99.1 % net loss). These results agree with the values  
460 presented in (Tesi et al., 2016). For the other compounds analyzed 55-74 % are associated  
461 with the fine fraction even for the shallowest station and they therefore experience sorting to  
462 a lesser extent.

463 Degradation after burial is assumed to play only a minor role. Differences in sedimentation  
464 ages are expected to be small (Section 2.1) and a study on centennial-scale sediment cores  
465 from the East Siberian Sea (Bröder et al., 2016) detected no significant TerrOC degradation  
466 (as recorded by biomarker loss) with increasing sediment depth. Also in that study, lignin  
467 phenol and cutin acid loadings were on average 20 times higher on the inner than on the  
468 outer shelf, whereas for HMW *n*-alkanoic acids and *n*-alkanes the difference between inner  
469 and outer shelf was only a factor of ~3-5. Contrasts between the stations were found to be  
470 larger than down-core changes. This may be due to the fact that the cores in that study only  
471 encompassed about one century of sedimentation ages, while the protracted cross-shelf  
472 transport likely requires much longer timescales.

473

### 474 3.2.2 Lignin Phenol sources

475 Relative distributions of different lignin phenol classes reveal more information on TerrOC  
476 sources since they are specific to different plant types. Syringyl phenols are not produced by  
477 gymnosperm (non-flowering) plants; elevated syringyl to vanillyl ratios (i.e. S/V > 1, Hedges  
478 and Parker, 1976) are therefore attributed to more lignin phenols from angiosperm  
479 (flowering) plants. These ratios have to be handled with care, though, because the  
480 preferential degradation of syringyl phenols by white- and brown-rot fungi on land can also  
481 alter S/V ratios (Hedges et al., 1988). S/V values for the Laptev Sea transect increased with  
482 increasing water depth from ~0.65 for the inner shelf to ~1.0 for the slope/rise sediments  
483 (Fig. 5A). This trend can either be explained by preferential degradation of gymnosperm  
484 material or sorting during transport. Tesi et al. (2014) measured generally lower values for  
485 S/V (ESAS average: 0.47, for only Lena watershed dominated locations: 0.42) recording no  
486 trend with water depth (Fig. S1 for comparisons with other studies). Their deepest station

487 was located at only 69 m water depth, though, whereas in this study sediments from down to  
488 3146 m water depth were analyzed. S/V ratios in Buor-Khaya Bay surface sediments  
489 (Winterfeld et al., 2015a) were also lower ( $0.43 \pm 0.02$  on average) and displayed no trend  
490 with water depth. Within the water depth interval they studied (5.8-17 m), however, the  
491 samples analyzed in this study had also quite homogeneous S/V ratios ( $0.64 \pm 0.02$ ). Two  
492 sediment cores from the East Siberian Sea (Bröder et al., 2016) showed also lower S/V  
493 values (inner shelf surface sediment: 0.62, outer shelf surface sediment: 0.50) displaying no  
494 clear trends over time/down-core. For the Beaufort Sea shelf Goñi et al. (2000) detected  
495 rather high values (0.54-1.71), which (besides the very high value at 61 m water depth)  
496 agree with the data from this study. Other transects across the North American Arctic margin  
497 (Goni et al., 2013) had slightly lower S/V ratios with no observed trends with water depth.  
498 The ratio of cinnamyl to vanillyl phenols (C/V) is associated with the relative contributions of  
499 woody versus soft material, because only non-woody vascular plants synthesize cinnamyl  
500 phenols (Hedges and Mann, 1979a). This ratio admittedly decreases with ongoing  
501 degradation (Opsahl and Benner, 1995) and may therefore not be used as an unambiguous  
502 source indicator. We observed that C/V values strongly decreased across the Laptev Sea  
503 Shelf from  $\sim 0.5$  (close to the Lena River outlet) to  $\sim 0.1$  (on the slope/rise, Fig. 5B), which  
504 may reflect the preferential degradation of soft tissues. This trend is not likely caused by  
505 hydrodynamic sorting, since typically the larger, low-density, woody plant fragments are  
506 retained in shallower water, whereas finer material is transported further across the shelf  
507 (e.g. Keil et al., 1994; Tesi et al., 2016).

508 C/V ratios in Buor-Khaya Bay sediments (Winterfeld et al., 2015a) in shallow waters were on  
509 average lower and more homogeneous ( $0.17 \pm 0.03$ ) than those measured in this study ( $0.41$   
510  $\pm 0.12$  for the corresponding depth interval) (Fig. S1 for comparisons with other studies). C/V  
511 values for the entire ESAS were on average 0.15 ( $0.14 \pm 0.07$  for only Lena dominated  
512 waters) with no water depth trend (Tesi et al., 2014). In shallow sediment cores from the East  
513 Siberian Sea, Bröder et al. (2016) measured C/V ratios of 0.20 (inner shelf) and 0.13 (outer  
514 shelf) for the surface sediments with no significant trend over sediment depth. For the

515 Mackenzie Shelf C/V values ranged between 0.16 and 0.32 and slightly increased with  
516 increasing water depth (Goñi et al., 2000). In contrast, in the Bering Sea, Chuckchi Sea,  
517 Barrow Canyon, Canadian Archipelago, Lancaster sound and Davis Strait there were no C/V  
518 trends observed (Goni et al., 2013), with lower values in the Canadian part ( $0.10 \pm 0.12$ ) and  
519 highest values on the Beaufort Sea slope, where values slightly decreased with increasing  
520 depth ( $0.39 \pm 0.07$ ).

521 A comparison to the S/V-C/V signatures of potential Arctic plant end-members (compiled by  
522 Amon et al., 2012, and citations therein, Tesi et al., 2014, and Winterfeld et al., 2015a)  
523 showed that lignin phenols likely derive from both angio- and gymnosperm soft tissues in the  
524 shallower samples, closely matching with willow (*Salix*) tissues measured by Winterfeld et al.  
525 (2015a). With increasing water depths, angiosperm wood became the most important source  
526 material, while gymnosperm wood, grasses and mosses did not appear to contribute  
527 significantly to the overall lignin phenol fingerprint (Fig. 5C). As discussed earlier, this trend  
528 may well be a result of preferential degradation and sorting during cross-shelf transport and  
529 not derive from actual changes in source material.

530

### 531 3.3 Degradation status of organic matter

532 During degradation, syringyl and vanillyl phenol aldehydes are oxidized to carboxylic acids of  
533 the same phenol group. Increasing Sd/SI and Vd/VI ratios can therefore qualitatively indicate  
534 ongoing degradation of lignin phenols (Ertel and Hedges, 1984; Hedges et al., 1988). For  
535 fresh plant material typical acid-to-aldehyde ratios are around 0.1-0.2 (Hedges et al., 1988).  
536 Winterfeld et al. (2015a), however, found values as high as Sd/SI = 0.80 and Vd/VI = 0.67 for  
537 a moss species (*Aulacomnium turgidum*), Sd/SI = 0.87 for larch (*Larix*) needles and Sd/SI =  
538 0.49 Vd/VI = 0.41 for wild rosemary (*Ledum palustre*). Sedges (*Carex spp.*), dwarf birch  
539 (*Betula nana*) and willow (*Salix*) range between Sd/SI = 0.13-0.24 and Vd/VI = 0.18-0.23.  
540 The ratio of CuO oxidation-derived 3,5-dihydroxybenzoic acid to vanillyl phenols (3,5-Bd/V)  
541 also serves as a proxy for degradation as 3,5-Bd is formed during humification likely  
542 occurring in soils (Gordon and Goñi, 2004; Hedges et al., 1988; Prahl et al., 1994; Tesi et al.,

2014). For this reason, this proxy can trace mineral rich soil organic matter in contrast to vascular plant debris (e.g. Dickens et al., 2007; Prah1 et al., 1994) as well as degradation during cross shelf transport (Tesi et al., 2016).

Sd/SI, Vd/VI and 3,5-Bd/V all increased along the transect, implying more degraded material with increasing residence time in the shelf system (Fig. 6A). There appeared to be no differences between outer shelf/slope and rise, which may indicate that TerrOC on the slope is already highly reworked. In contrast, Tesi et al. (2014) found no correlation between Sd/SI or Vd/VI and distance from the coast, while 3,5-Bd/V significantly increased with increasing distance from the coast (Fig. S2 for comparisons with other studies). Sd/SI values for the Buor-Khaya Bay from Winterfeld et al. (2015a) were slightly higher ( $1.04 \pm 0.24$ ) than samples from the corresponding water depths in this study ( $0.66 \pm 0.15$ ), whereas Vd/VI values were significantly higher ( $1.28 \pm 0.30$  compared to  $0.59 \pm 0.14$ ). Measurements for the Mackenzie Shelf agreed with the ones in this study (Sd/SI =  $0.81 \pm 0.25$  compared to  $1.01 \pm 0.33$  for the corresponding water depths; Vd/VI =  $0.69 \pm 0.14$  to  $0.86 \pm 0.26$ ; 3,5-Bd/V =  $0.19 \pm 0.04$  to  $0.31 \pm 0.15$ ), but did not show a trend with water depth (Goñi et al., 2000).

Tesi et al. (2016) observed lower acid/aldehyde ratios for the lignin-rich low-density fraction compared to the other fractions (high-density with different grain sizes and settling velocities) in coastal surface sediments from the ESAS. With increasing distance from the coast, these values increased, whereas for the other fractions there were no apparent trends. These findings were interpreted as relatively fresh lignin in the low-density fraction (rich in large plant fragments) compared to the relatively degraded lignin that had likely experienced leaching and adsorbed to the fine mineral fractions (i.e. mineral bound OC). Bulk 3,5-Bd/V values are potentially affected by both sorting and degradation, as they increased with decreasing particle size (fine and ultrafine fractions had the most degraded signal and are preferentially transported to the outer shelf) and across the shelf in each of the fractions.

The carbon preference indices for HMW *n*-alkanes and HMW *n*-alkanoic acids have also been widely applied as degradation proxies for plant waxes in marine sediments (for the ESAS, e.g. van Dongen et al., 2008; Fahl and Stein, 1997; Fernandes and Sicre, 2000; Vonk

571 et al., 2010). It measures the ratio of odd-to-even numbers of carbon chain-lengths of HMW  
572 lipids and is based on the preference of odd carbon chain-lengths for HMW *n*-alkanes in  
573 fresh plant material (even carbon chain-lengths for HMW *n*-alkanoic acids; Eglinton and  
574 Hamilton, 1967). With ongoing degradation this preference is lost and the CPI approaches 1  
575 (Bray and Evans, 1961).

576 We observed that the HMW *n*-alkane CPI presented a similar pattern as the lignin phenol  
577 based degradation indices. However, the HMW *n*-alkanoic acid CPI did not show as much of  
578 a degradation trend (HMW *n*-alkane CPI: ~5.7 close to the coast, ~2.2 for the deep stations;  
579 HMW *n*-alkanoic acids: ~5.4 close to the coast, ~4.1 for the deep stations; Fig. 6B). Karlsson  
580 et al. (2011) measured lipid CPIs in the Buor-Khaya Bay with 10-80 km distance to the coast  
581 and obtained similar results to this ~800 km cross-shelf study, with higher values closer to  
582 the river delta (Fig. S2 for comparisons with other studies). Their data appears to have a  
583 wider spread, though, which might be due to either the narrower dynamic range. Fahl and  
584 Stein (1997) also reported a large range of *n*-alkane CPI values (< 0.2- > 5) for Laptev Sea  
585 sediments. Fernandes and Sicre (2000) analyzed sediments from the Kara Sea and from the  
586 major rivers discharging into this sea, Ob and Yenisey rivers. In the marine environment and  
587 the Ob River, they observed HMW *n*-alkane CPI values between 4.8 and 5.3, similar to those  
588 found at shallow water depths in this study. For the Yenisey River and mixing zone, they  
589 found higher CPI values, pointing to fresher material being transported there. Vonk et al.  
590 (2010) recorded HMW *n*-alkane CPI values for sediments along the East Siberian Sea  
591 Kolyma paleoriver transect (across the East Siberian Sea) shelf that decreased from > 7.5 to  
592 < 4.0 with increasing distance from the river mouth, overall higher than in this study but  
593 confirming the general trend to more degraded material on the outer shelf. Tesi et al. (2016)  
594 found HMW *n*-alkanoic acid CPI values to decrease with decreasing particle size with no  
595 significant trends across the shelf in all but the low-density fraction, which is largely retained  
596 close to the shore. The HMW *n*-alkane CPI values in that study, however, showed no  
597 systematical differences between different fractions, but an overall decreasing trend with  
598 increasing distance from the coast.



599 When undergoing degradation, HMW *n*-alkanoic acids may also lose their functional groups,  
600 turning them into HMW *n*-alkanes (Meyers and Ishiwatari, 1993). The slightly decreasing  
601 ratio of HMW *n*-alkanoic acids to *n*-alkanes also hints at more degraded material with  
602 increasing water depth, although, due to a rather large variability, this trend is not significant.  
603 For the Buor-Khaya Bay surface sediments Karlsson et al. (2011) obtained similar results  
604 (0.48-10.7, here 1.1-10.9) with higher values closer to the river delta (Fig. S2 for  
605 comparisons with other studies). Along the Kolyma paleoriver transect, Vonk et al. (2010)  
606 measured HMW *n*-alkanoic acid to *n*-alkane ratios between 1 and 6 with no clear trend with  
607 increasing distance from the river mouth. Tesi et al. (2016) found decreasing values with  
608 increasing distance from the coast with no differences between the fractions. Two sediment  
609 cores from inner and outer East Siberian Sea recording about one century of sedimentation  
610 showed no clear trend in CPI or HMW *n*-alkanoic acid/*n*-alkane towards more degraded  
611 TerrOC with increasing sediment depth (Bröder et al., 2016), but displayed a similar  
612 difference between inner and outer shelf as seen in this study. This contrasting behavior for  
613 cross-shelf and down-core trends may be caused by significantly different timescales for the  
614 two processes: about one century in situ/after burial compared to potentially several millennia  
615 long lateral transport. Furthermore, the degradation efficiency is likely higher under the oxic  
616 conditions prevailing during cross-shelf lateral transport (Keil et al., 2004), than in the anoxic  
617 conditions that predominate below a few millimeters of sediments on the ESAS (e.g. Boetius  
618 and Damm, 1998). Comparing in situ to transport-related oxygen exposure times on the wide  
619 Arctic shelves could potentially resolve the observed discrepancies.

#### 620 **4 Concluding remarks and future research directions**

621 Across the Laptev Sea from the Lena River mouth to the deep sea of the Arctic interior a  
622 considerable loss of terrigenous organic matter has been observed on both bulk and  
623 molecular level. All terrigenous biomarkers display a massive decline with increasing water  
624 depth along this high-resolution transect due to hydrodynamic sorting and degradation during  
625 transport. Terrigenous organic matter (TerrOC) seems to be also qualitatively more degraded  
626 on the outer shelf, slope and rise compared to inner shelf and coastal areas.

627 These results corroborate and expand previous findings for the East Siberian Arctic Shelf,  
628 showing that the shelf seas in this region function as an active reactor for TerrOC. Since the  
629 East Siberian Arctic Shelf belongs to the widest and shallowest continental margins on Earth,  
630 cross-shelf transport times and thus the time spent in oxic sediments are expected to be  
631 comparatively long. This stands in contrast to e.g. the Mackenzie basin, which is thought to  
632 act as a geological sink for organic carbon due to its TerrOC burial (Hilton et al., 2015). For  
633 narrower Arctic shelves in general, where transport times can be expected to be much  
634 shorter, organic matter transfer towards the deeper basins appears to be much more  
635 efficient, with high TerrOC concentrations in surface sediments even at greater water depths  
636 (e.g. Barrow Canyon, Goni et al., 2013). It can therefore be assumed that the cross-shelf  
637 transport time exerts first-order control over the extent of TerrOC degradation. With ongoing  
638 global warming, rising permafrost-derived organic carbon input from river-sediment discharge  
639 and coastal erosion is expected to reach the marine environment. It is therefore crucial to  
640 better constrain cross-shelf transport times in order to determine a TerrOC degradation rate  
641 and thereby contribute to quantifying potential carbon-climate feedbacks.

642

#### 643 **Acknowledgements**

644 We thank crew and personnel of the IB *ODEN*, the RV *Yakob Smirnitskyi* and the *TB0012*.  
645 The SWERUS-C3 and the International Siberian Shelf Study 2008 (ISSS-08) expeditions  
646 were supported by the Knut and Alice Wallenberg Foundation, Headquarters of the Far

647 Eastern Branch of the Russian Academy of Sciences, the Swedish Research Council (VR  
648 Contract No. 621-2004-4039, 621-2007-4631 and 621-2013-5297), the US National Oceanic  
649 and Atmospheric Administration (OAR Climate Program Office, NA08OAR4600758/Siberian  
650 Shelf Study), the Russian Foundation of Basic Research RFFI (08-05-13572, 08-05-00191-a,  
651 and 07-05-00050a), the Swedish Polar Research Secretariat, the Nordic Council of Ministers  
652 and the US National Science Foundation (OPP ARC 0909546). L. Bröder also acknowledges  
653 financial support from the Climate Research School of the Bolin Climate Research Centre. T.  
654 Tesi also acknowledges EU financial support as a Marie Curie fellow (contract no. PIEF-GA-  
655 2011-300259), contribution no. ~~XXXX-1900~~ of ISMAR-CNR Sede di Bologna. J.A. Salvadó  
656 also acknowledges EU financial support as a Marie Curie grant (FP7-PEOPLE-2012-IEF;  
657 project 328049). I. Semiletov thanks the Russian Government for financial support (mega-  
658 grant #14.Z50.31.0012). O. Dudarev thanks the Russian Science Foundation (grant No. 15-  
659 17-20032). Furthermore we would like thank Francien Peterse, Xiaojuan Feng and one  
660 anonymous reviewer for their constructive comments, which helped to improve this  
661 manuscript.

662 **References**

- 663 Aller, R. C. and Blair, N. E.: Carbon remineralization in the Amazon-Guianas tropical mobile mudbelt: A  
664 sedimentary incinerator, *Continental Shelf Research*, 26(17-18), 2241–2259, doi:10.1016/j.csr.2006.07.016, 2006.
- 665 Amon, R. M. W., Rinehart, A. J., Duan, S., Louchouart, P., Prokushkin, A., Guggenberger, G., Bauch, D.,  
666 Stedmon, C., Raymond, P. A., Holmes, R. M., McClelland, J. W., Peterson, B. J., Walker, S. A. and Zhulidov, A.  
667 V.: Dissolved organic matter sources in large Arctic rivers, *Geochimica et Cosmochimica Acta*, 94, 217–237,  
668 doi:10.1016/j.gca.2012.07.015, 2012.
- 669 Belicka, L. L., Macdonald, R. W., Yunker, M. B. and Harvey, H. R.: The role of depositional regime on carbon  
670 transport and preservation in Arctic Ocean sediments, *Marine Chemistry*, 86(1-2), 65–88,  
671 doi:10.1016/j.marchem.2003.12.006, 2004.
- 672 Blair, N. E. and Aller, R. C.: The Fate of Terrestrial Organic Carbon in the Marine Environment, *Annual Review of*  
673 *Marine Science*, 4(1), 401–423, doi:10.1146/annurev-marine-120709-142717, 2012.
- 674 Boetius, A. and Damm, E.: Benthic oxygen uptake, hydrolytic potentials and microbial biomass at the Arctic  
675 continental slope, *Deep-Sea Research Part I: Oceanographic Research Papers*, 45(2-3), 239–275,  
676 doi:10.1016/S0967-0637(97)00052-6, 1998.
- 677 Boetius, A., Albrecht, S., Bakker, K., Bienhold, C., Felden, J., Fernández-Méndez, M., Hendricks, S., Katlein, C.,  
678 Lalande, C., Krumpfen, T., Nicolaus, M., Peeken, I., Rabe, B., Rogacheva, A., Rybakova, E., Somavilla, R. and  
679 Wenzhöfer, F.: Export of algal biomass from the melting Arctic sea ice., *Science (New York, N.Y.)*, 339(6126),  
680 1430–2, doi:10.1126/science.1231346, 2013.
- 681 Bray, E. . and Evans, E. .: Distribution of n-paraffins as a clue to recognition of source beds, *Geochimica et*  
682 *Cosmochimica Acta*, 22(1), 2–15, doi:10.1016/0016-7037(61)90069-2, 1961.
- 683 Brunauer, S., Emmett, P. H. and Teller, E.: Adsorption of Gases in Multimolecular Layers, *Journal of the*  
684 *American Chemical Society*, 60(2), 309–319, doi:citeulike-article-id:4074706rdoi: 10.1021/ja01269a023, 1938.
- 685 Bröder, L., Tesi, T., Andersson, A., Eglinton, T. I., Semiletov, I. P., Dudarev, O. V., Roos, P. and Gustafsson, Ö.:  
686 Historical records of organic matter supply and degradation status in the East Siberian Sea, *Organic*  
687 *Geochemistry*, 91, 16–30, doi:10.1016/j.orggeochem.2015.10.008, 2016.
- 688 Charkin, A. N., Dudarev, O. V., Semiletov, I. P., Kruhmalev, A. V., Vonk, J. E., Sánchez-García, L., Karlsson, E.,  
689 Gustafsson, O., Gustafsson, Ö. and Gustafsson, O.: Seasonal and interannual variability of sedimentation and  
690 organic matter distribution in the Buor-Khaya Gulf: The primary recipient of input from Lena River and coastal  
691 erosion in the southeast Laptev Sea, *Biogeosciences*, 8(9), 2581–2594, doi:10.5194/bg-8-2581-2011, 2011.
- 692 Dethleff, D.: Entrainment and export of Laptev Sea ice sediments, Siberian Arctic, *Journal of Geophysical*  
693 *Research C: Oceans*, 110(7), 1–17, doi:10.1029/2004JC002740, 2005.
- 694 Dethleff, D.: Dense water formation in the Laptev Sea flaw lead, *Journal of Geophysical Research: Oceans*,  
695 115(12), 1–16, doi:10.1029/2009JC006080, 2010.
- 696 Dickens, A. F., Gudeman, J. A., Gélinas, Y., Baldock, J. A., Tinner, W., Hu, F. S. and Hedges, J. I.: Sources and  
697 distribution of CuO-derived benzene carboxylic acids in soils and sediments, *Organic Geochemistry*, 38(8), 1256–  
698 1276, doi:10.1016/j.orggeochem.2007.04.004, 2007.
- 699 Dmitrenko, I. A., Kirillov, S. A. and Bruno Tremblay, L.: The long-term and interannual variability of summer fresh  
700 water storage over the eastern Siberian shelf: Implication for climatic change, *Journal of Geophysical Research:*  
701 *Oceans*, 113(3), 1–14, doi:10.1029/2007JC004304, 2008.
- 702 Eglinton, G. and Hamilton, R. J.: Leaf epicuticular waxes., *Science (New York, N.Y.)*, 156(780), 1322–1335,  
703 doi:10.1126/science.156.3780.1322, 1967.
- 704 Eicken, H., Reimnitz, E., Alexandrov, V., Martin, T., Kassens, H. and Viehoff, T.: Sea-ice processes in the Laptev  
705 Sea and their importance for sediment export, *Continental Shelf Research*, 17(2), 205–233, doi:10.1016/S0278-  
706 4343(96)00024-6, 1997.
- 707 Ertel, J. R. and Hedges, J. I.: The lignin component of humic substances: Distribution among soil and sedimentary  
708 humic, fulvic, and base-insoluble fractions, *Geochimica et Cosmochimica Acta*, 48(10), 2065–2074,  
709 doi:10.1016/0016-7037(84)90387-9, 1984.
- 710 Fahl, K. and Stein, R.: Modern organic carbon deposition in the Laptev Sea and the adjacent continental slope:

- 711 Surface water productivity vs. terrigenous input, *Organic Geochemistry*, 26(5-6), 379–390, doi:10.1016/S0146-  
712 6380(97)00007-7, 1997.
- 713 Feng, X., Vonk, J. E., van Dongen, B. E., Gustafsson, Ö., Semiletov, I. P., Dudarev, O. V., Wang, Z., Montluçon,  
714 D. B., Wacker, L. and Eglinton, T. I.: Differential mobilization of terrestrial carbon pools in Eurasian Arctic river  
715 basins., *Proceedings of the National Academy of Sciences of the United States of America*, 110(35), 14168–73,  
716 doi:10.1073/pnas.1307031110, 2013.
- 717 Feng, X., Gustafsson, Ö., Holmes, R. M., Vonk, J. E., van Dongen, B. E., Semiletov, I. P., Dudarev, O. V.,  
718 Yunker, M. B., Macdonald, R. W., Montluçon, D. B. and Eglinton, T. I.: Multi-molecular tracers of terrestrial carbon  
719 transfer across the pan-Arctic – Part 1: Comparison of hydrolysable components with plant wax lipids and lignin  
720 phenols, *Biogeosciences Discussions*, 12(6), 4721–4767, doi:10.5194/bgd-12-4721-2015, 2015.
- 721 Fernandes, M. B. and Sicre, M. A.: The importance of terrestrial organic carbon inputs on Kara Sea shelves as  
722 revealed by n-alkanes, OC and d13C values, in *Organic Geochemistry*, vol. 31, pp. 363–374., 2000.
- 723 Fry, B. and Sherr, E. B.: d13C Measurements as indicators of carbon flow in marine and freshwater ecosystems,  
724 *Contributions in Marine Science*, 27, 13–49, 1984.
- 725 Goni, M. A., O'Connor, A. E., Kuzyk, Z. Z., Yunker, M. B., Gobeil, C. and Macdonald, R. W.: Distribution and  
726 sources of organic matter in surface marine sediments across the North American Arctic margin, *Journal of*  
727 *Geophysical Research-Oceans*, 118(9), 4017–4035, doi:10.1002/jgrc.20286, 2013.
- 728 Goñi, M. A. and Hedges, J. I.: Sources and reactivities of marine-derived organic matter in coastal sediments as  
729 determined by alkaline CuO oxidation, *Geochimica et Cosmochimica Acta*, 59(14), 2965–2981, doi:10.1016/0016-  
730 7037(95)00188-3, 1995.
- 731 Goñi, M. A. and Montgomery, S.: Alkaline CuO oxidation with a microwave digestion system: Lignin analyses of  
732 geochemical samples, *Analytical Chemistry*, 72(14), 3116–3121, doi:10.1021/ac991316w, 2000.
- 733 Goñi, M. A., Ruttenger, K. C. and Eglinton, T. I.: A reassessment of the sources and importance of land-derived  
734 organic matter in surface sediments from the Gulf of Mexico, *Geochimica et Cosmochimica Acta*, 62(18), 3055–  
735 3075, doi:10.1016/S0016-7037(98)00217-8, 1998.
- 736 Goñi, M. A., Yunker, M. B., MacDonald, R. W. and Eglinton, T. I.: Distribution and sources of organic biomarkers  
737 in arctic sediments from the Mackenzie River and Beaufort Shelf, *Marine Chemistry*, 71(1-2), 23–51,  
738 doi:10.1016/S0304-4203(00)00037-2, 2000.
- 739 Gordeev, V. V.: Fluvial sediment flux to the Arctic Ocean, *Geomorphology*, 80(1-2), 94–104,  
740 doi:10.1016/j.geomorph.2005.09.008, 2006.
- 741 Gordon, E. S. and Goñi, M. A.: Controls on the distribution and accumulation of terrigenous organic matter in  
742 sediments from the Mississippi and Atchafalaya river margin, *Marine Chemistry*, 92(1-4 SPEC. ISS.), 331–352,  
743 doi:10.1016/j.marchem.2004.06.035, 2004.
- 744 Guay, C. K. H., Falkner, K. K., Muench, R. D., Mensch, M., Frank, M. and Bayer, R.: Wind-driven transport for  
745 Eurasian Arctic river discharge, *Journal of Geophysical Research*, 106(C6), 11469–11480, 2001.
- 746 Gustafsson, Ö., Van Dongen, B. E., Vonk, J. E., Dudarev, O. V. and Semiletov, I. P.: Widespread release of old  
747 carbon across the Siberian Arctic echoed by its large rivers, *Biogeosciences*, 8(6), 1737–1743, doi:10.5194/bg-8-  
748 1737-2011, 2011.
- 749 Günther, F., Overduin, P. P., Sandakov, A. V., Grosse, G. and Grigoriev, M. N.: Short- and long-term thermo-  
750 erosion of ice-rich permafrost coasts in the Laptev Sea region, *Biogeosciences*, 10(6), 4297–4318,  
751 doi:10.5194/bg-10-4297-2013, 2013.
- 752 Hedges, J. I. and Mann, D. C.: The characterization of plant tissues by their lignin oxidation products, *Geochimica*  
753 *et Cosmochimica Acta*, 43(11), 1803–1807, doi:10.1016/0016-7037(79)90028-0, 1979a.
- 754 Hedges, J. I. and Mann, D. C.: The lignin geochemistry of marine sediments from the southern Washington coast,  
755 *Geochimica et Cosmochimica Acta*, 43(11), 1809–1818, doi:10.1016/0016-7037(79)90029-2, 1979b.
- 756 Hedges, J. I. and Parker, P. L.: Land-derived organic matter in surface sediments from the Gulf of Mexico,  
757 *Geochimica et Cosmochimica Acta*, 40, 1019–1029, 1976.
- 758 Hedges, J. I., Blanchette, R. A., Weliky, K. and Devol, A. H.: Effects of fungal degradation on the CuO oxidation  
759 products of lignin: A controlled laboratory study, *Geochimica et Cosmochimica Acta*, 52(11), 2717–2726,  
760 doi:10.1016/0016-7037(88)90040-3, 1988.

- 761 Hilton, R. G., Galy, V., Gaillardet, J., Dellinger, M., Bryant, C., O'Regan, M., Gröcke, D. R., Coxall, H., Bouchez, J.  
762 and Calmels, D.: Erosion of organic carbon in the Arctic as a geological carbon dioxide sink, *Nature*, 524(7563),  
763 84–87, doi:10.1038/nature14653, 2015.
- 764 Holmes, R. M., McClelland, J. W., Peterson, B. J., Shiklomanov, I. A., Shiklomanov, A. I., Zhulidov, A. V.,  
765 Gordeev, V. V and Bobrovitskaya, N. N.: A circumpolar perspective on fluvial sediment flux to the Arctic ocean,  
766 *Global Biogeochemical Cycles*, 16(4), 14–45, doi:10.1029/2001GB001849, 2002.
- 767 Holmes, R. M., McClelland, J. W., Peterson, B. J., Tank, S. E., Bulygina, E., Eglinton, T. I., Gordeev, V. V.,  
768 Gurtovaya, T. Y., Raymond, P. a., Repeta, D. J., Staples, R., Striegl, R. G., Zhulidov, A. V. and Zimov, S. a.:  
769 Seasonal and Annual Fluxes of Nutrients and Organic Matter from Large Rivers to the Arctic Ocean and  
770 Surrounding Seas, *Estuaries and Coasts*, 35(2), 369–382, doi:10.1007/s12237-011-9386-6, 2012.
- 771 Hugelius, G., Strauss, J., Zubrzycki, S., Harden, J. W., Schuur, E. A. G., Ping, C. L., Schirmer, L., Grosse, G.,  
772 Michaelson, G. J., Koven, C. D., O'Donnell, J. A., Elberling, B., Mishra, U., Camill, P., Yu, Z., Palmtag, J. and  
773 Kuhry, P.: Improved estimates show large circumpolar stocks of permafrost carbon while quantifying substantial  
774 uncertainty ranges and identifying remaining data gaps, *Biogeosciences Discussions*, 11(3), 4771–4822,  
775 doi:10.5194/bgd-11-4771-2014, 2014.
- 776 Ivanov, V. V. and Golovin, P. N.: Observations and modeling of dense water cascading from the northwestern  
777 Laptev Sea shelf, *Journal of Geophysical Research: Oceans*, 112(9), 1–15, doi:10.1029/2006JC003882, 2007.
- 778 Jakobsson, M., Grantz, A., Kristoffersen, Y. and Macnab, R.: Physiography and Bathymetry of the Arctic Ocean,  
779 in *The Organic Carbon Cycle in the Arctic Ocean*, edited by R. Stein and R. W. Macdonald, pp. 1–5., 2004.
- 780 Karlsson, E. S., Charkin, A., Dudarev, O., Semiletov, I., Vonk, J. E., Sánchez-García, L. and Andersson, A.:  
781 Carbon isotopes and lipid biomarker investigation of sources, transport and degradation of terrestrial organic  
782 matter in the Buor-Khaya Bay, SE Laptev Sea, *Biogeosciences*, 8(7), 1865–1879, doi:10.5194/bg-8-1865-2011,  
783 2011.
- 784 Karlsson, E. S., Brüchert, V., Tesi, T., Charkin, a, Dudarev, O., Semiletov, I. and Gustafsson, Ö.: Contrasting  
785 regimes for organic matter degradation in the East Siberian Sea and the Laptev Sea assessed through microbial  
786 incubations and molecular markers, *Marine Chemistry*, 170, 11–22, doi:10.1016/j.marchem.2014.12.005, 2014.
- 787 Keil, R. G., Tsamakis, E., Fuh, C. B., Giddings, J. C. and Hedges, J. I.: Mineralogical and textural controls on the  
788 organic composition of coastal marine sediments: Hydrodynamic separation using SPLITT-fractionation,  
789 *Geochimica et Cosmochimica Acta*, 58(2), 879–893, doi:10.1016/0016-7037(94)90512-6, 1994.
- 790 Keil, R. G., Mayer, L. M., Quay, P. D., Richey, J. E. and Hedges, J. I.: Loss of organic matter from riverine  
791 particles in deltas, *Geochimica et Cosmochimica Acta*, 61(7), 1507–1511, doi:10.1016/S0016-7037(97)00044-6,  
792 1997a.
- 793 Keil, R. G., Tsamakis, E. and Wolf, N.: Relationships between organic carbon preservation and mineral surface  
794 area in Amazon fan sediments (Holes 932A and 942A), *Proceedings of the Ocean Drilling Program*, 155, 531–  
795 538 [online] Available from: <http://cat.inist.fr/?aModele=afficheN&cpsid=2169716>, 1997b.
- 796 Keil, R. G., Dickens, A. F., Arnarson, T., Nunn, B. L. and Devol, A. H.: What is the oxygen exposure time of  
797 laterally transported organic matter along the Washington margin?, *Marine Chemistry*, 92(1-4 SPEC. ISS.), 157–  
798 165, doi:10.1016/j.marchem.2004.06.024, 2004.
- 799 Macdonald, R. W., Naidu, A. S., Yunker, M. B. and Gobeil, C.: The Beaufort Sea: distribution, sources, fluxes and  
800 burial of organic carbon, in *The Organic Carbon Cycle in the Arctic Ocean*, edited by R. Stein and R. W.  
801 Macdonald, pp. 177–192., 2004.
- 802 Magen, C., Chaillou, G., Crowe, S. a., Mucci, A., Sundby, B., Gao, A., Makabe, R. and Sasaki, H.: Origin and fate  
803 of particulate organic matter in the southern Beaufort Sea - Amundsen Gulf region, *Canadian Arctic, Estuarine,  
804 Coastal and Shelf Science*, 86(1), 31–41, doi:10.1016/j.ecss.2009.09.009, 2010.
- 805 Mammine, K. A.: Sediment provenance and transport on the Siberian Arctic shelf, Oregon State University.,  
806 1998.
- 807 Mayer, L. M.: Surface area control of organic carbon accumulation in continental shelf sediments, *Geochimica et  
808 Cosmochimica Acta*, 58(4), 1271–1284, doi:10.1016/0016-7037(94)90381-6, 1994.
- 809 Mayer, L., Benninger, L., Bock, M., DeMaster, D., Roberts, Q. and Martens, C.: Mineral associations and  
810 nutritional quality of organic matter in shelf and upper slope sediments off Cape Hatteras, USA: A case of  
811 unusually high loadings, *Deep-Sea Research Part II: Topical Studies in Oceanography*, 49(20), 4587–4597,  
812 doi:10.1016/S0967-0645(02)00130-3, 2002.

- 813 McClelland, J. W., Holmes, R. M., Peterson, B. J., Amon, R., Brabets, T., Cooper, L., Gibson, J., Gordeev, V. V.,  
814 Guay, C., Milburn, D., Staples, R., Raymond, P. A., Shiklomanov, I., Stiegl, R., Zhulidov, A., Gurtovaya, T. and  
815 Zimov, S.: Development of a Pan-Arctic Database for River Chemistry From Corals to Canyons : The Great  
816 Barrier Reef Margin, Program, 89(24), 217–218, doi:10.1029/2006JG000353., 2008.
- 817 Mercone, D., Thomson, J., Abu-Zied, R. H., Croudace, I. W. and Rohling, E. J.: High-resolution geochemical and  
818 micropalaeontological profiling of the most recent eastern Mediterranean sapropel, *Marine Geology*, 177(1-2), 25–  
819 44, doi:10.1016/S0025-3227(01)00122-0, 2001.
- 820 Meyers, P. A. and Ishiwatari, R.: Lacustrine organic geochemistry-an overview of indicators of organic matter  
821 sources and diagenesis in lake sediments, *Organic Geochemistry*, 20(7), 867–900, doi:10.1016/0146-  
822 6380(93)90100-P, 1993.
- 823 Naidu, A. S., Cooper, L. W., Finney, B. P., Macdonald, R. W., Alexander, C. and Semiletov, I. P.: Organic carbon  
824 isotope ratio (d13C) of Arctic Amerasian Continental shelf sediments, *International Journal of Earth Sciences*,  
825 89(3), 522–532, doi:10.1007/s005310000121, 2000.
- 826 Nieuwenhuize, J., Maas, Y. E. . and Middelburg, J. J.: Rapid analysis of organic carbon and nitrogen in particulate  
827 materials, *Marine Chemistry*, 45(3), 217–224, doi:10.1016/0304-4203(94)90005-1, 1994.
- 828 Opsahl, S. and Benner, R.: Early diagenesis of vascular plant tissues : Lignin and cutin decomposition and  
829 biogeochemical implications, *Geochimica et Cosmochimica Acta*, 59(23), 4889–4904, 1995.
- 830 Panova, E., Tesi, T., Pearce, C., Salvadó, J. A., Karlsson, E. S., Kruså, M., Semiletov, I. P. and Gustafsson, Ö.:  
831 Geochemical compositional differences of the supramicron plankton-dominated fraction in two regimes of the  
832 Marginal Ice Zone (MIZ) of the outer East Siberian Arctic Shelf, in AGU Fall Meeting, p. Conference Abstract  
833 C43A–0797., 2015.
- 834 Pearson, A., Mcnichol, A. P., Schneider, R. J., von Reden, K. F. and Zheng, Y.: Microscale AMS 14C  
835 measurement at NOSAMS, *Radiocarbon*, 40(1), 61–75, 1998.
- 836 Prah, F. G., Ertel, J. R., Goni, M. A., Sparrow, M. A. and Eversmeyer, B.: Terrestrial organic carbon contributions  
837 to sediments on the Washington margin, *Geochimica et Cosmochimica Acta*, 58(14), 3035–3048,  
838 doi:10.1016/0016-7037(94)90177-5, 1994.
- 839 Rachold, V. and Hubberten, H. W.: Carbon isotope composition of particulate organic material in east Siberian  
840 rivers, *Land-Ocean Systems in the Siberian Arctic: Dynamics and History*, 223–238, 1998.
- 841 Rachold, V., Grigoriev, M. N., Are, F. E., Solomon, S., Reimnitz, E., Kassens, H. and Antonow, M.: Coastal  
842 erosion vs riverine sediment discharge in the Arctic Shelf seas, *International Journal of Earth Sciences*, 89(3),  
843 450–459, doi:10.1007/s005310000113, 2000.
- 844 Rachold, V., Eicken, H., Gordeev, V. V., Grigoriev, M. N., Hubberten, H.-W., Lisitzin, A. P., Shevchenko, V. P. and  
845 Schirrmeister, L.: Modern Terrigenous Organic Carbon Input to the Arctic Ocean, *The Organic  
846 Carbon Cycle in the Arctic Ocean*, 33–55, 2004.
- 847 Sakshaug, E.: Primary and secondary production in the Arctic Seas, in *The Organic Carbon Cycle in the Arctic  
848 Ocean*, edited by R. Stein and R. W. Macdonald, pp. 57–81., 2004.
- 849 Salvadó, J. A., Tesi, T., Andersson, A., Ingri, J., Dudarev, O. V., Semiletov, I. P. and Gustafsson, Ö.: Organic  
850 carbon remobilized from thawing permafrost is resequenced by reactive iron on the Eurasian Arctic Shelf,  
851 *Geophysical Research Letters*, 42(19), 8122–8130, doi:10.1002/2015GL066058, 2015.
- 852 Sánchez-García, L., Alling, V., Pugach, S., Vonk, J., Van Dongen, B., Humborg, C., Dudarev, O., Semiletov, I.  
853 and Gustafsson, Ö.: Inventories and behavior of particulate organic carbon in the Laptev and East Siberian seas,  
854 *Global Biogeochemical Cycles*, 25(2), 1–13, doi:10.1029/2010GB003862, 2011.
- 855 Schubert, C. J. and Calvert, S. E.: Nitrogen and carbon isotopic composition of marine and terrestrial organic  
856 matter in Arctic Ocean sediments:, *Deep Sea Research Part I: Oceanographic Research Papers*, 48(3), 789–810,  
857 doi:10.1016/S0967-0637(00)00069-8, 2001.
- 858 Semiletov, I.P., Destruction of the coastal permafrost ground as an important factor in biogeochemistry of the  
859 Arctic Shelf waters, *Trans. (Doklady) Russian Acad. Sci.*, 368, 679-682, 1999 (translated into English).
- 860 Semiletov, I. and Gustafsson, Ö.: East Siberian Shelf Study Alleviates Scarcity of Observations, *Eos*,  
861 *Transactions American Geophysical Union*, 90(17), 145, doi:10.1029/2009EO170001, 2009.
- 862 Semiletov, I., Dudarev, O., Luchin, V., Charkin, A., Shin, K. H. and Tanaka, N.: The East Siberian Sea as a

- 863 transition zone between Pacific-derived waters and Arctic shelf waters, *Geophysical Research Letters*, 32(10), 1–  
864 5, doi:10.1029/2005GL022490, 2005.
- 865 Semiletov, I. P., Pipko, I. I., Shakhova, N. E., Dudarev, O. V., Pugach, S. P., Charkin, A. N., Mroy, C. P.,  
866 Kosmach, D. and Gustafsson, Ö.: Carbon transport by the Lena River from its headwaters to the Arctic Ocean,  
867 with emphasis on fluvial input of terrestrial particulate organic carbon vs. carbon transport by coastal erosion,  
868 *Biogeosciences*, 8(9), 2407–2426, doi:10.5194/bg-8-2407-2011, 2011.
- 869 Semiletov, I. P., Shakhova, N. E., Sergienko, V. I., Pipko, I. I. and Dudarev, O. V.: On carbon transport and fate in  
870 the East Siberian Arctic land–shelf–atmosphere system, *Environmental Research Letters*, 7(1), 015201,  
871 doi:10.1088/1748-9326/7/1/015201, 2012.
- 872 Semiletov, I. P., Shakhova, N. E., Pipko, I. I., Pugach, S. P., Charkin, A. N., Dudarev, O. V., Kosmach, D. A. and  
873 Nishino, S.: Space-time dynamics of carbon and environmental parameters related to carbon dioxide emissions in  
874 the Buor-Khaya Bay and adjacent part of the Laptev Sea, *Biogeosciences*, 10(9), 5977–5996, doi:10.5194/bg-10-  
875 5977-2013, 2013.
- 876 Semiletov, I., Pipko, I., Gustafsson, Ö., Anderson, L. G., Sergienko, V., Pugach, S., Dudarev, O., Charkin, A.,  
877 Gukov, A., Bröder, L., Andersson, A., Spivak, E. and Shakhova, N.: Acidification of East Siberian Arctic Shelf  
878 waters through addition of freshwater and terrestrial carbon, *Nature Geoscience*, (April), doi:10.1038/NEGO2695,  
879 2016.
- 880 Shakhova, N., Semiletov, I., Sergienko, V., Lobkovsky, L., Yusupov, V., Salyuk, A., Salomatin, A., Chernykh, D.,  
881 Kosmach, D., Panteleev, G., Nicolsky, D., Samarkin, V., Joye, S., Charkin, A., Dudarev, O., Meluzov, A. and  
882 Gustafsson, O.: The East Siberian Arctic Shelf: towards further assessment of permafrost-related methane fluxes  
883 and role of sea ice., *Philosophical transactions. Series A, Mathematical, physical, and engineering sciences*,  
884 373(2052), 20140451–, doi:10.1098/rsta.2014.0451, 2015.
- 885 Stein, R. and Fahl, K.: Holocene accumulation of organic carbon at the Laptev Sea continental margin (Arctic  
886 Ocean): sources, pathways, and sinks, *Geo-Marine Letters*, 20(1), 27–36, doi:10.1007/s003670000028, 2000.
- 887 Stein, R. and Fahl, K.: The Laptev Sea: Distribution, Sources, Variability and Burial of Organic Carbon, in *The*  
888 *Organic Carbon Cycle in the Arctic Ocean*, edited by R. Stein and R. W. Macdonald, pp. 213–236., 2004.
- 889 Stein, R. and Macdonald, R. W., Eds.: *The organic carbon cycle in the Arctic Ocean*, Springer Verlag., 2004.
- 890 Stuvier, M. and Polach, H. A.: Reporting of 14C Data, *Radiocarbon*, 19(3), 355–363,  
891 doi:10.1016/j.forsciint.2010.11.013, 1977.
- 892 Syvitski, J. P. M.: Sediment discharge variability in Arctic rivers: Implications for a warmer future, *Polar Research*,  
893 21(2), 323–330, doi:10.1111/j.1751-8369.2002.tb00087.x, 2002.
- 894 Tarnocai, C., Canadell, J. G., Schuur, E. A. G., Kuhry, P., Mazhitova, G. and Zimov, S.: Soil organic carbon pools  
895 in the northern circumpolar permafrost region, *Global Biogeochemical Cycles*, 23(2), 1–11,  
896 doi:10.1029/2008GB003327, 2009.
- 897 Tesi, T., Semiletov, I., Hugelius, G., Dudarev, O., Kuhry, P. and Gustafsson, Ö.: Composition and fate of  
898 terrigenous organic matter along the Arctic land-ocean continuum in East Siberia: Insights from biomarkers and  
899 carbon isotopes, *Geochimica et Cosmochimica Acta*, 133, 235–256, doi:10.1016/j.gca.2014.02.045, 2014.
- 900 Tesi, T., Semiletov, I., Dudarev, O., Andersson, A. and Gustafsson, Ö.: Matrix association effects on  
901 hydrodynamic sorting and degradation of terrestrial organic matter during cross-shelf transport in the Laptev and  
902 East Siberian shelf seas, *Journal of Geophysical Research: Biogeosciences*, 121(3), 731–752,  
903 doi:10.1002/2015JG003067, 2016.
- 904 van Dongen, B. E., Semiletov, I., Weijers, J. W. H. and Gustafsson, Ö.: Contrasting lipid biomarker composition of  
905 terrestrial organic matter exported from across the Eurasian Arctic by the five great Russian Arctic rivers, *Global*  
906 *Biogeochemical Cycles*, 22(1), 1–14, doi:10.1029/2007GB002974, 2008a.
- 907 van Dongen, B. E., Zencak, Z. and Gustafsson, Ö.: Differential transport and degradation of bulk organic carbon  
908 and specific terrestrial biomarkers in the surface waters of a sub-arctic brackish bay mixing zone, *Marine*  
909 *Chemistry*, 112(3-4), 203–214, doi:10.1016/j.marchem.2008.08.002, 2008b.
- 910 Vonk, J. E. and Gustafsson, Ö.: Permafrost-carbon complexities, *Nature Geoscience*, 6(9), 675–676,  
911 doi:10.1038/ngeo1937, 2013.
- 912 Vonk, J. E., Sánchez-García, L., Semiletov, I., Dudarev, O., Eglinton, T., Andersson, A. and Gustafsson, O.:



913 Molecular and radiocarbon constraints on sources and degradation of terrestrial organic carbon along the Kolyma  
914 paleoriver transect, East Siberian Sea, *Biogeosciences*, 7(10), 3153–3166, doi:10.5194/bg-7-3153-2010, 2010.

915 Vonk, J. E., Sánchez-García, L., van Dongen, B. E., Alling, V., Kosmach, D., Charkin, A., Semiletov, I. P.,  
916 Dudarev, O. V., Shakhova, N., Roos, P., Eglinton, T. I., Andersson, A. and Gustafsson, Ö.: Activation of old  
917 carbon by erosion of coastal and subsea permafrost in Arctic Siberia, *Nature*, 489(7414), 137–140,  
918 doi:10.1038/nature11392, 2012.

919 Vonk, J. E., Semiletov, I. P., Dudarev, O. V., Eglinton, T. I., Andersson, A., Shakhova, N., Charkin, A., Heim, B.  
920 and Gustafsson, Ö.: Preferential burial of permafrost-derived organic carbon in Siberian-Arctic shelf waters,  
921 *Journal of Geophysical Research: Oceans*, 119, 8410–8421, doi:10.1002/2014JC010261. Received, 2014.

922 Wegner, C., Hölemann, J. A., Dmitrenko, I., Kirillov, S. and Kassens, H.: Seasonal variations in Arctic sediment  
923 dynamics - Evidence from 1-year records in the Laptev Sea (Siberian Arctic), *Global and Planetary Change*, 48(1-  
924 3 SPEC. ISS.), 126–140, doi:10.1016/j.gloplacha.2004.12.009, 2005.

925 Wegner, C., Bauch, D., Hölemann, J. A., Janout, M. A., Heim, B., Novikhin, A., Kassens, H. and Timokhov, L.:  
926 Interannual variability of surface and bottom sediment transport on the Laptev Sea shelf during summer,  
927 *Biogeosciences*, 10(2), 1117–1129, doi:10.5194/bg-10-1117-2013, 2013.

928 Weingartner, T. J., Danielson, S., Sasaki, Y., Pavlov, V. and Kulakov, M.: The Siberian Coastal Current: A wind-  
929 and buoyancy-forced Arctic coastal current, *Journal of Geophysical Research*, 104(C12), 29697,  
930 doi:10.1029/1999JC900161, 1999.

931 Wiesenberg, G. L. B., Schwark, L. and Schmidt, M. W. I.: Improved automated extraction and separation  
932 procedure for soil lipid analyses, *European Journal of Soil Science*, 55(2), 349–356, doi:10.1111/j.1351-  
933 0754.2004.00601.x, 2004.

934 Winterfeld, M., Goñi, M. A., Just, J., Hefter, J. and Mollenhauer, G.: Characterization of particulate organic matter  
935 in the Lena River Delta and adjacent nearshore zone, NE Siberia - Part 2: Lignin-derived phenol compositions,  
936 *Biogeosciences*, 12, 2261–2283, doi:10.5194/bgd-11-14359-2014, 2015a.

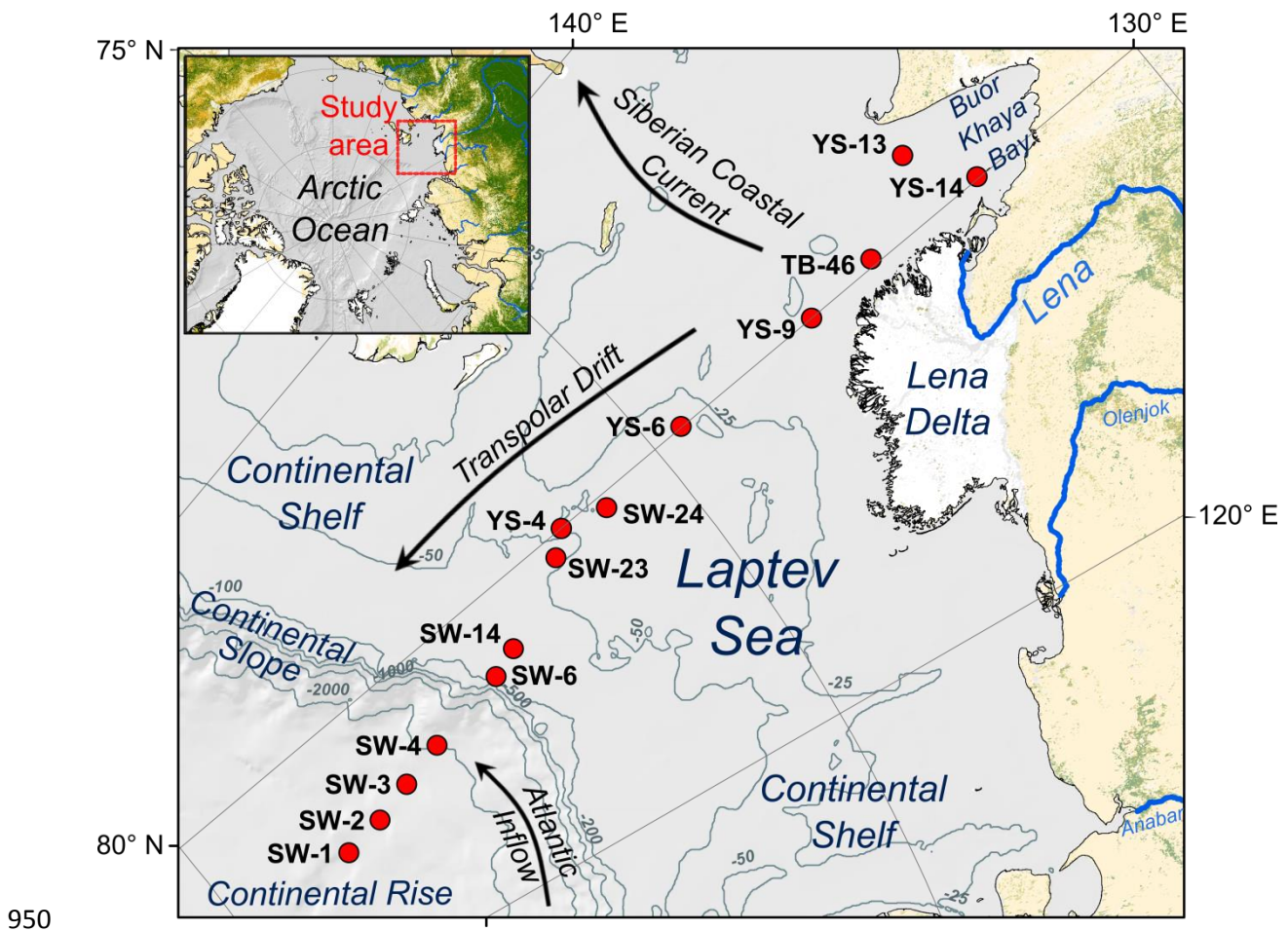
937 Winterfeld, M., Laepple, T. and Mollenhauer, G.: Characterization of particulate organic matter in the Lena River  
938 delta and adjacent nearshore zone, NE Siberia - Part I: Radiocarbon inventories, *Biogeosciences*, 12(12), 3769–  
939 3788, doi:10.5194/bg-12-3769-2015, 2015b.

940 Yunker, M. B., Macdonald, R. W., Cretney, W. J., Fowler, B. R., Mclaughlin, F. A. and Bay, R. R. B.: Alkane,  
941 terpene, and polycyclic aromatic hydrocarbon geochemistry of the Mackenzie River and Mackenzie shelf."  
942 Riverine contributions to Beaufort Sea coastal sediment, , 57, 3041–3061, 1993.

943 Yunker, M. B., Macdonald, R. W., Veltkamp, D. J. and Cretney, W. J.: Terrestrial and marine biomarkers in a  
944 seasonally ice-covered Arctic estuary — integration of multivariate and biomarker approaches, *Marine Chemistry*,  
945 49(1), 1–50, doi:http://dx.doi.org/10.1016/0304-4203(94)00057-K, 1995.

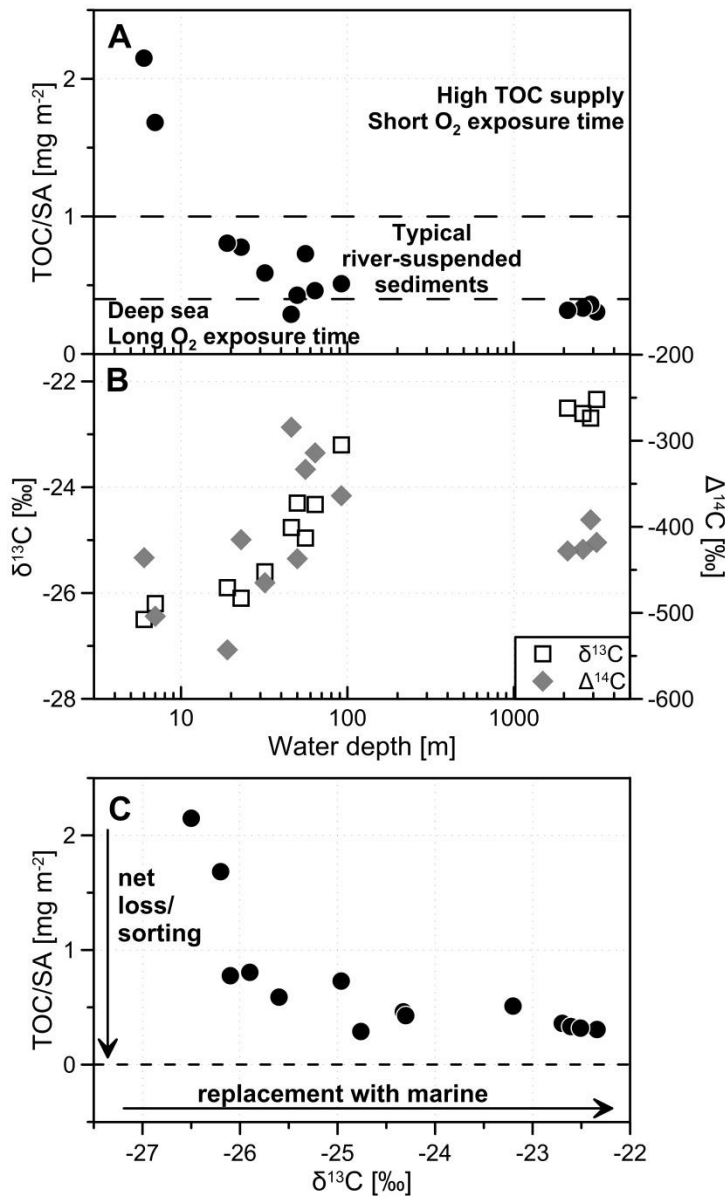
946 Yunker, M. B., Belicka, L. L., Harvey, H. R. and Macdonald, R. W.: Tracing the inputs and fate of marine and  
947 terrigenous organic matter in Arctic Ocean sediments: A multivariate analysis of lipid biomarkers, *Deep-Sea  
948 Research Part II: Topical Studies in Oceanography*, 52(24-26), 3478–3508, doi:10.1016/j.dsr2.2005.09.008, 2005.

949

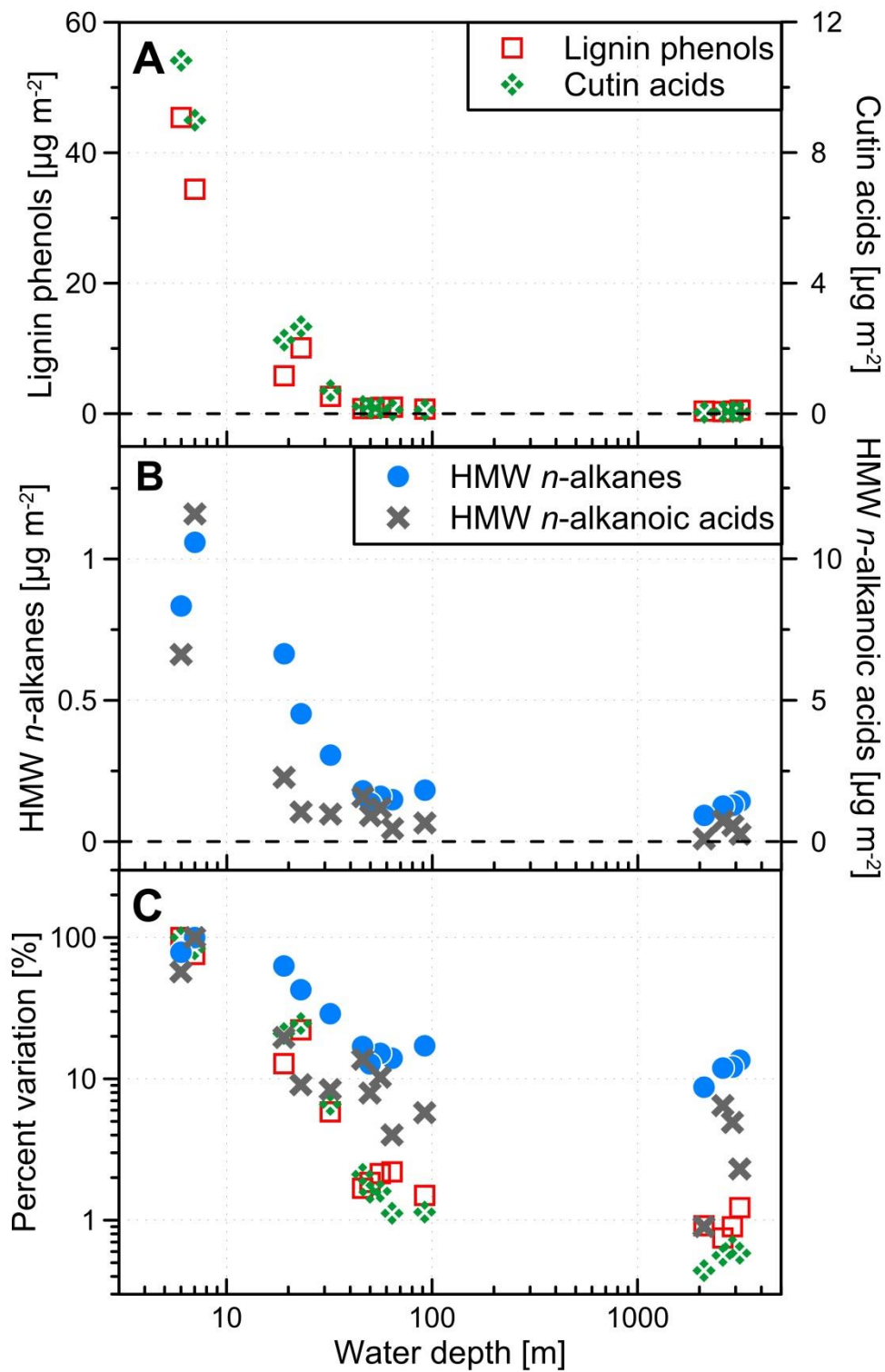


950

951 Figure 1: Map of the study area in the Laptev Sea. Red filled circles mark the sediment  
 952 sampling sites. The transect reaches from the Lena River mouth and the Buor-Khaya Bay  
 953 (water depths ~10 m) across the Laptev Sea Shelf (mean depth ~50 m) to the slope/shelf  
 954 break and rise (water depths ~3000 m). Arrows show the directions of the prevailing ocean  
 955 currents.

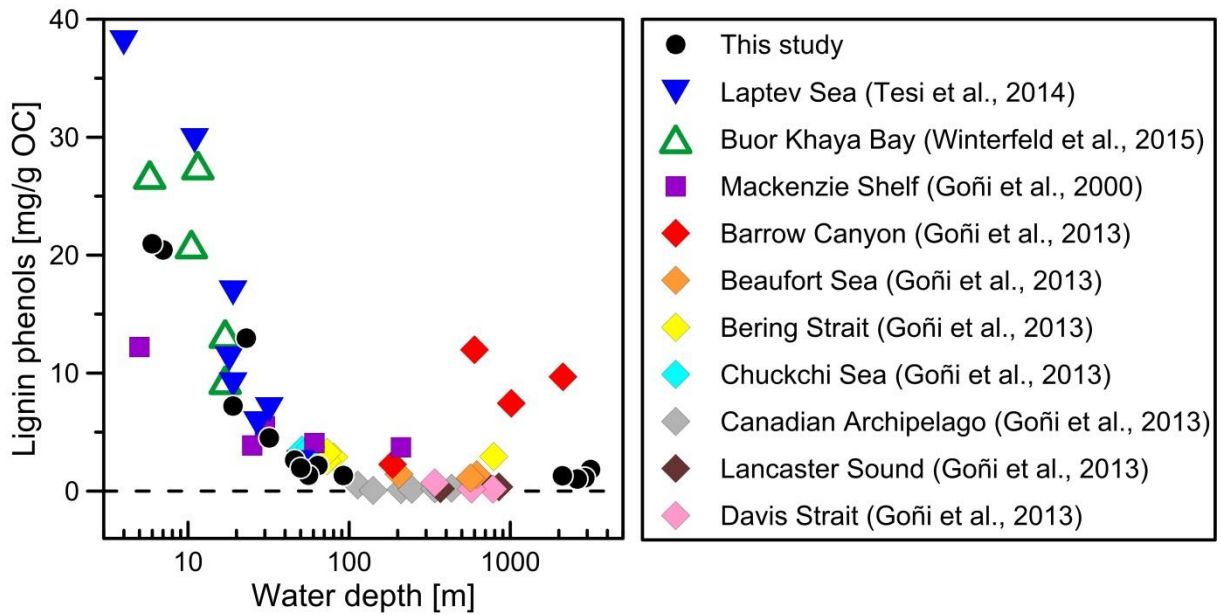


956  
 957 Figure 2: (A) The ratio of total organic carbon (TOC) to mineral surface area (SA). Typical  
 958 values for deep sea, river-suspended sediments and high TOC supply are taken from Blair  
 959 and Aller (2012). (B) The stable carbon isotopic signal ( $\delta^{13}\text{C}$ , open boxes) and the  
 960 radiocarbon isotopic signal ( $\Delta^{14}\text{C}$ , filled diamonds). (C) The relationship between TOC/SA  
 961 and  $\delta^{13}\text{C}$  can help to disentangle two processes occurring simultaneously during cross-shelf  
 962 transport: The net loss (i.e. degradation) or sorting (i.e. hydraulically retaining) of TerrOC  
 963 leads to a shift towards lower TOC/SA ratios, whereas the replacement/dilution with marine  
 964 OC shifts the isotopic signature towards higher values.



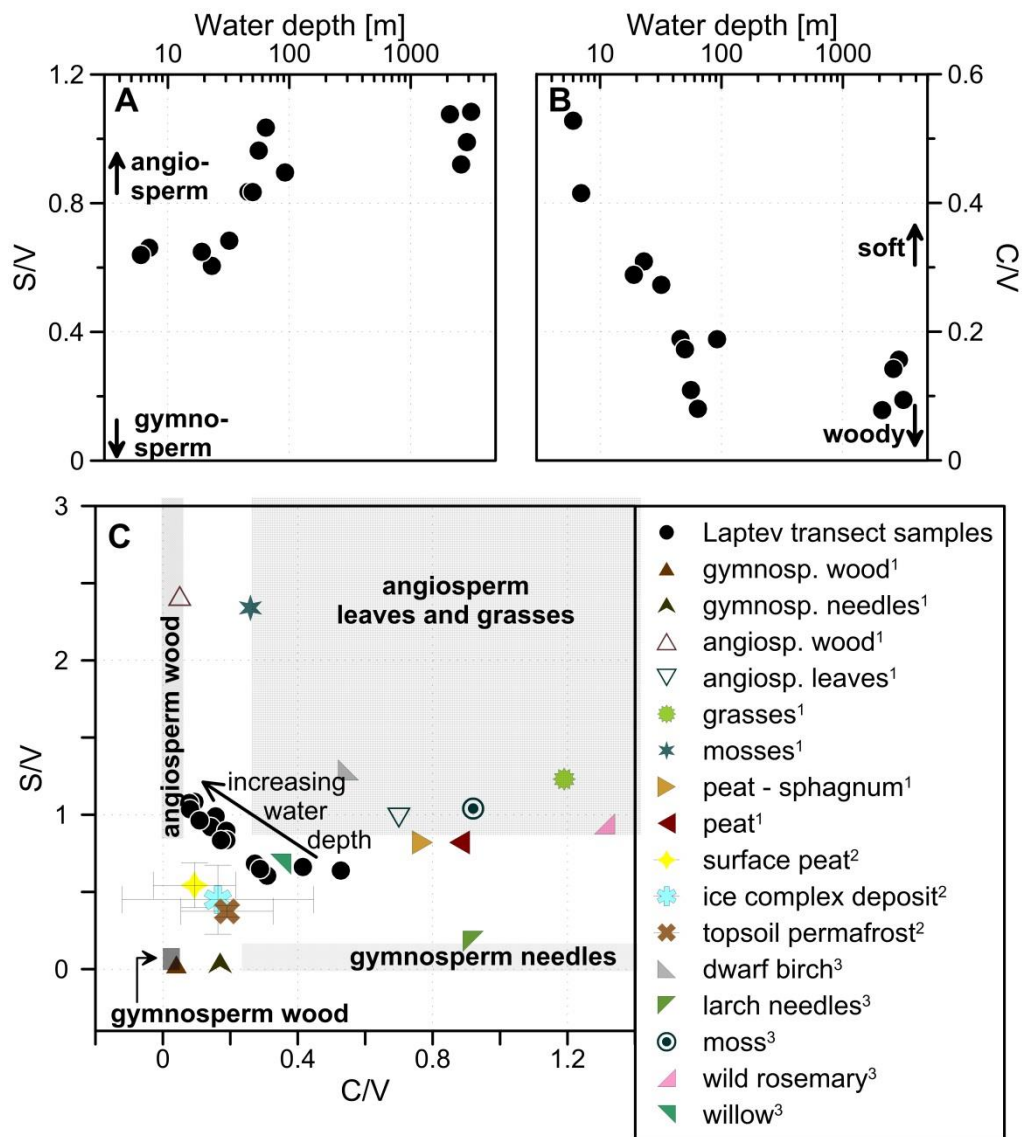
965

966 Figure 3: Terrigenous biomarker loadings across the shelf: (A) lignin phenols and cutin acids,  
 967 (B) HMW *n*-alkanes and HMW *n*-alkanoic acids. (C) Comparison between the different  
 968 biomarkers along the transect: lignin phenols, cutin acids, HMW *n*-alkanoic acids and *n*-  
 969 alkanes where each is normalized to respective highest value (corresponding to 100 %).



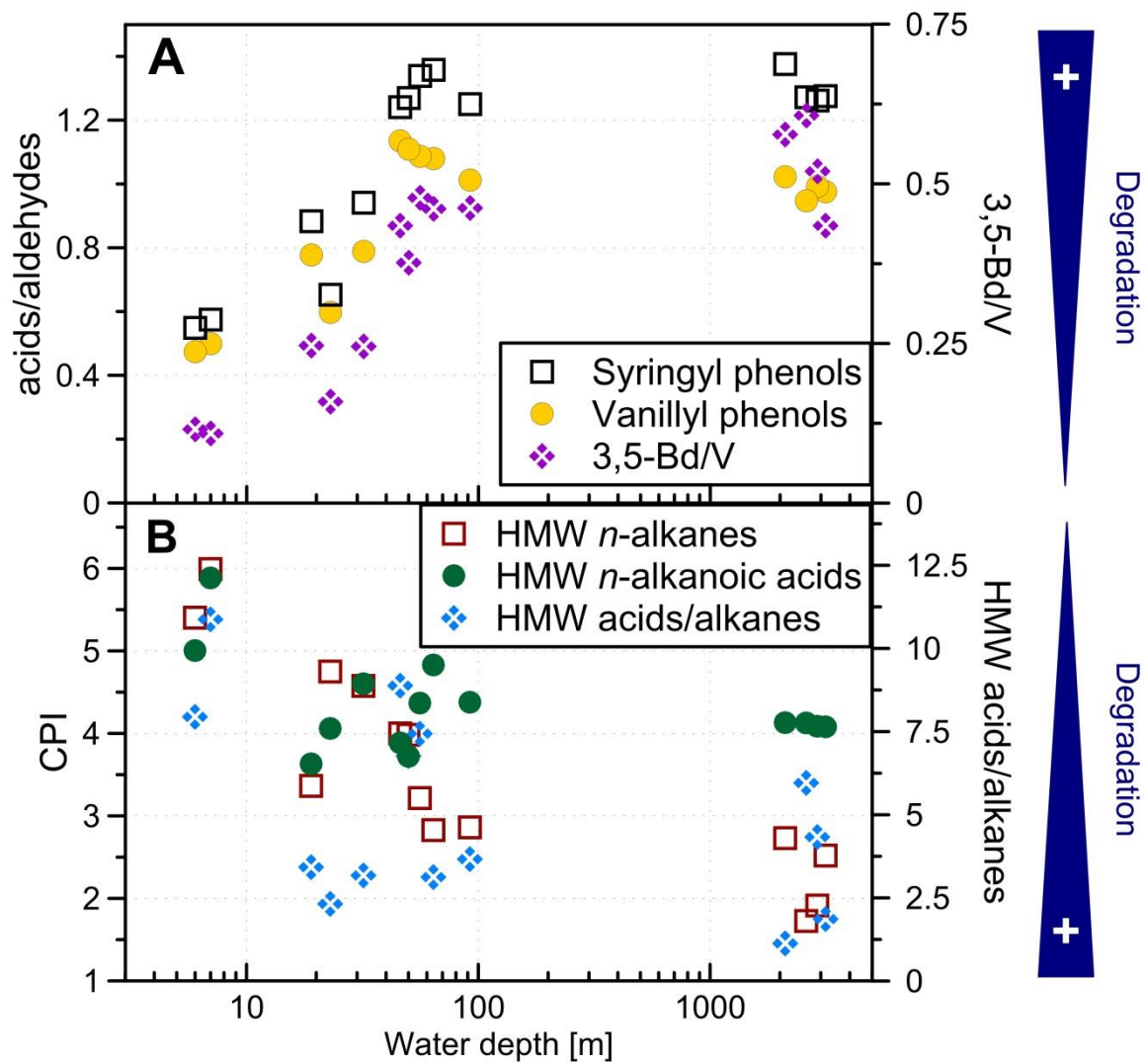
970

971 Figure 4: A comparison of lignin phenol data from this project to values from published  
972 studies around the Arctic Ocean. Similar decreasing trends with increasing water depth are  
973 observed for all systems but Barrow Canyon, where elevated lignin phenols concentrations  
974 are found even at depth of > 1000 m.



975

976 Figure 5: The lignin phenol composition carries source information: (A) an increasing ratio of  
 977 syringyl to vanillyl phenols (S/V) suggests relatively more angiosperm material. (B) A  
 978 decreasing ratio of cinnamyl to vanillyl phenols (C/V) implies an increasing relative  
 979 contribution of woody material compared to soft tissues. (C) Comparison of S/V and C/V with  
 980 the end-members for different Arctic plants as compiled from different studies by Amon et al.  
 981 (2012, and citations therein, here marked with <sup>1</sup>); ice-complex deposit and topsoil permafrost  
 982 as determined by Tesi et al. (2014, here marked with <sup>2</sup>) and more plant species measured by  
 983 Winterfeld et al. (2015a, here marked with <sup>3</sup>). The boxes indicate typical ranges of S/V and  
 984 C/V for different vascular plant tissues in different locations (e.g. Goñi et al., 2000).



985

986 Figure 6: Degradation proxies for TerrOC, blue triangles point toward lower extent of  
 987 degradation: (A) CuO-oxidation derived ratios Sd/SI, Vd/VI and 3,5-Bd/V. (B) Carbon  
 988 preference indices (CPI) of HMW *n*-alkanes and *n*-alkanoic acids and the ratio of HMW *n*-  
 989 alkanolic acids to HMW *n*-alkanes.

990

991 **Table 1: List of surface sediment samples from the Laptev Sea transect**

ID	Sample type	Lat	Long	Water depth	OC	SA	$\delta^{13}\text{C}$	$\Delta^{14}\text{C}$	SiO <sub>2</sub>	Al <sub>2</sub> O <sub>3</sub>	CaO
		° N	° E	m	mg g <sup>-1</sup>	m <sup>2</sup> g <sup>-1</sup>	‰	‰	wt %	wt %	wt %
S W-1	0-0.5cm	78.942	125.243	3146	10.4	34.0	-22.34	-418	60.3	16.5	2.4
S W-2	0-0.5cm	78.581	125.607	2900	13.8	38.3	-22.70	-392	57.8	17.2	2.1
S W-3	0-0.5cm	78.238	126.150	2601	10.6	31.8	-22.64	-426	62.1	16.0	1.6
S W-4	0-0.5cm	77.855	126.664	2106	13.2	41.5	-22.54	-428	56.6	17.5	1.3
S W-6	0-1cm	77.142	127.378	92	7.6	14.9	-23.20	-364	72.0	12.6	1.7
S W-14	0-1cm	76.894	127.798	64	8.9	19.4	-24.33	-314	71.3	12.5	1.5
S W-23	0-1cm	76.171	129.333	56	15.8	21.7	-25.04-96	-333	68.9	13.6	1.4
Y S-4	0-1cm	75.987	129.984	50	13.4 <sup>a</sup>	31.4	-24.876 <sup>a</sup>	-284 <sup>a</sup>	63.8	15.1	1.3
S W-24	0-1cm	75.599	129.558	46	10.7	37.0	-24.30	-437	62.5	15.4	1.2
Y S-6	0-1cm	74.724	130.016	32	18.6 <sup>a</sup>	31.6	-25.60 <sup>a</sup>	-465 <sup>a</sup>	62.1	16.1	1.3
Y S-9	Grab	73.366	129.997	23	13.1 <sup>b</sup>	16.9	-26.10 <sup>b</sup>	-415 <sup>b</sup>	70.8	14.0	1.3
Y S-13	0-1cm	71.968	131.701	19	18.9 <sup>a</sup>	23.5	-25.90 <sup>a</sup>	-543 <sup>a</sup>	61.6	17.4	0.8
Y S-14	0-1cm	71.630	130.050	7	19.1 <sup>a</sup>	11.4	-26.20 <sup>a</sup>	-504 <sup>a</sup>	69.6	15.0	1.6
T B-46	Grab	72.700	130.180	6	25.8 <sup>a</sup>	12.0 <sup>c</sup>	-26.50 <sup>a</sup>	-436 <sup>a</sup>	67.9	15.2	1.8

992

993 <sup>a</sup> Data from Vonk et al. (2012); <sup>b</sup> data from Tesi et al. (2016); <sup>c</sup> data from Karlsson et al.  
 994 (2014).



995 **Table 2: Biomarker results for surface sediment samples from the Laptev Sea transect**

ID	Lignin $\mu\text{g m}^{-2}$	Cutin $\mu\text{g m}^{-2}$	HMW* alkanes $\mu\text{g m}^{-2}$	HMW** acids $\mu\text{g m}^{-2}$	S/V	C/V	Sd/SI	Vd/VI	3,5Bd/V	CPI alk	CPI acids alk	acids/ alk
SW-1	0.56	0.063	0.14	0.27	1.1	0.09	1.3	0.98	0.43	2.5	4.1	1.9
SW-2	0.41	0.070	0.13	0.57	0.99	0.16	1.3	0.99	0.52	1.9	4.1	4.3
SW-3	0.34	0.061	0.13	0.75	0.92	0.14	1.3	0.95	0.61	1.7	4.1	6.0
SW-4	0.42	0.048	0.093	0.10	1.1	0.08	1.4	1.0	0.58	2.7	4.1	1.1
SW-6	0.68	0.12	0.18	0.67	0.90	0.19	1.2	1.0	0.46	2.9	4.4	3.7
SW-14	1.0	0.12	0.15	0.46	1.0	0.08	1.4	1.1	0.46	2.8	4.8	3.1
SW-23	0.97	0.17	0.16	1.2	0.96	0.11	1.3	1.1	0.48	3.2	4.4	7.4
YS-4	0.84	0.17	0.13	0.92	0.83	0.17	1.3	1.1	0.38	4.0	3.7	6.8
SW-24	0.76	0.23	0.18	1.6	0.84	0.19	1.2	1.1	0.43	4.0	3.9	8.9
YS-6	2.7	0.71	0.31	0.97	0.68	0.27	0.94	0.79	0.25	4.6	4.6	3.2
YS-9	10	2.7	0.45	1.1	0.60	0.31	0.65	0.60	0.16	4.7	4.1	2.3
YS-13	5.8	2.3	0.64	2.3	0.65	0.29	0.88	0.78	0.25	3.4	3.6	3.4
YS-14	34	9.0	1.1	12	0.66	0.42	0.57	0.50	0.11	6.0	5.9	11
TB-46	45	11	0.83 <sup>d</sup>	6.6 <sup>d</sup>	0.64	0.53	0.55	0.47	0.12	5.4 <sup>d</sup>	5.0 <sup>d</sup>	7.9 <sup>d</sup>

996

997 \* carbon chain-lengths 23-34; \*\* carbon chain-lengths 24-30.

998 <sup>d</sup> recalculated data from Karlsson et al. (2011).